Spring 2012

Gene Duplication and the Evolution of Hemoglobin Isoform Differentiation in Birds

Michael T. Grispo
University of Nebraska-Lincoln, mgrispo@gmail.com

Gene Duplication and the Evolution of Hemoglobin Isoform Differentiation in Birds

by

Michael T. Grispo

A THESIS

Presented to the Faculty of

The Graduate College at the University of Nebraska

In Partial Fulfillment of Requirements

For the Degree of Master of Science

Major: Biological Sciences

Under the Supervision of Professor Jay F. Storz

Lincoln, Nebraska

December, 2011

Gene Duplication and the Evolution of Hemoglobin Isoform Differentiation in Birds

Michael Thomas Grispo, M.S.

University of Nebraska, 2012

Adviser: Jay F. Storz

The majority of bird species co-express two functionally distinct hemoglobin (Hb) isoforms in definitive erythrocytes: HbA (the major adult Hb isoform, with α-chain subunits encoded by the α^A-globin gene) and HbD (the minor adult Hb isoform, with α-chain subunits encoded by the α^D-globin gene). The α^D-globin gene originated via tandem duplication of an embryonic α-like globin gene in the stem lineage of tetrapod vertebrates, which suggests the possibility that functional differentiation between the HbA and HbD isoforms may be attributable to a retained ancestral character state in HbD that harkens back to a primordial, embryonic function. To investigate this possibility and to examine other aspects of the evolution of the avian α-like globin genes, in collaborative effort with the Roy E. Weber lab, Joana Projecto-Garcia, Chandrasekhar Nataraja, and Hideaki Moriyama, we conducted a combined analysis of protein biochemistry and sequence evolution to characterize the structural and functional basis of Hb isoform differentiation in birds. The main objectives were: (1) to characterize the O_2-binding properties of HbA and HbD in species that are representative of several major avian lineages; (2) to gain insight into the possible structural basis of the observed functional differentiation between the HbA and HbD isoforms; and (3) to determine whether functional differentiation between the HbA and HbD isoforms is primarily attributable to post-duplication substitutions that occurred in the α^A- and α^D-globin gene

lineages, or whether the differentiation is attributable to substitutions that occurred in the single-copy, pre-duplication ancestor of the α^D- and α^E-globin genes, in which case the distinctive properties of HbD may represent a retained ancestral character state that is shared with embryonic Hb. Functional experiments involving purified HbA and HbD isofoms from 12 different bird species confirmed that HbD is characterized by a consistently higher O_2-affinity in the presence of allosteric effectors such as organic phosphates and Cl^- ions. In the case of both HbA and HbD, analyses of oxygenation properties under the two-state Monod-Wyman-Changeux allosteric model revealed that the pH-dependence of Hb-O_2 affinity stems from changes in the O_2 association constant of deoxy (T-state) Hb. Ancestral sequence reconstructions indicated that the replacement substitutions that distinguish the avian α^A- and α^D-globin genes occurred exclusively on post-duplication branches of the gene family phylogeny, suggesting that the observed functional differences between the HbA and HbD isoforms are not attributable to the retention of an ancestral (pre-duplication) character state in the α^D-globin gene.

Table of Contents

CHAPTER 1

1.1 Introduction

Hemoglobin (Hb) is one of the most extensively studied proteins in terms of structure-function relationships, and comparative studies of Hbs from nonhuman animals have made important contributions to this knowledge base (Dickerson and Geis 1983; Perutz 1983; Bunn and Forget 1986; Weber and Fago 2004). Despite this detailed understanding, a number of vexing questions about Hb function continue to challenge comparative biochemists and physiologists. One such question concerns the functional and adaptive significance of co-expressing multiple, structurally distinct Hb isoforms (isoHbs; Perutz 1983; Weber 1990, 1995, 2000; Ingermann 1997; Weber *et al.* 2000a). All or most vertebrate species express functionally distinct isoHbs during different stages of pre-natal development, and in many groups it is also common to co-express different isoHbs during postnatal life. The majority of birds and nonavian reptiles co-express two functionally distinct isoHbs in definitive erythrocytes: HbA (the major adult isoHb, with α-chain subunits encoded by the α^A-globin gene) and HbD (the minor adult isoHb, with α-chains encoded by the α^D-globin gene). HbD typically accounts for ~10-30% of total Hb in circulating erythrocytes, and available evidence indicates that it is generally characterized by an elevated O_2-affinity relative to HbA (Vandecasserie *et al.* 1973; Oberthür *et al.* 1983; Hiebl *et al.* 1988, 1989; Weber *et al.* 1988; Nothum *et al.* 1989; Tamburrini *et al.* 2000; Sanna *et al.* 2007).

Insights into the physiological division of labor between the HbA and HbD isoforms may help to explain why the duplicated α^A- and α^D-globin genes have been retained in the majority of birds and nonavian reptiles. Since the HbA and HbD isoforms exhibit consistent differences in O_2-binding properties, regulatory changes in intraerythrocytic isoHb stoichiometry could provide a mechanism for modulating blood-O_2 affinity in response to changes in O_2 availability or changes in internal metabolic demand (Lutz 1980). For example, in birds that experience

transitory hypoxia during ascent to high altitudes, it has been suggested that the co-expression of multiple isoHbs with graded O_2-affinities may expand the permissible range of arterial O_2 tensions for pulmonary/tissue O_2 transport (Hiebl *et al.* 1988; Weber *et al.* 1988). It is also possible that the physiological benefits of Hb heterogeneity are unrelated to O_2-binding properties. If isoHbs with different isoelectric points co-occur in the same erythrocytes, then Hb heterogeneity may enhance solubility (and hence, corpuscular Hb concentration), thereby increasing the O_2-carrying capacity of the blood (Perutz *et al.* 1959; Riggs 1976, 1979). IsoHbs with different charges would also indirectly influence the distribution of protons and other ions across the red cell membrane by altering the Donnan equilibrium, and this could play an important role in the allosteric regulation of Hb-O_2 affinity and cellular metabolism (Nikinmaa 2001; Jensen 2004). These considerations led Ingermann (1997:369) to conclude that it "…seems unlikely that the presence of electrophoretically distinguishable Hb multiplicity represents selectively neutral variations in Hb structure and function."

Available evidence suggests that the tetrapod common ancestor possessed three tandemly-linked gene duplicates that encode the α-chain subunits of the $\alpha_2\beta_2$ Hb tetramer: 5'-α^E-α^D-α^A-3' (Hoffmann and Storz 2007; Hoffmann *et al.* 2010; Storz *et al.* 2011a). In the stem lineage of tetrapods, the α^E- and α^A-globin genes originated via tandem duplication of an ancestral α-like globin gene, and α^D-globin originated subsequently via tandem duplication of the proto α^E-globin gene (Hoffmann and Storz 2007). In tetrapod vertebrates, the α^E-globin gene is exclusively expressed in larval/embryonic erythroid cells and the α^A-globin gene is expressed in definitive erythroid cells during later stages of prenatal development and postnatal life. In birds and nonavian reptiles that have been studied to date, the α^D-globin gene is expressed in both primitive and definitive erythroid cells (Cirotto *et al.* 1987; Alev *et al.* 2009; Storz *et al.* 2011b). HbD does not appear to be expressed in the definitive erythrocytes of crocodilians (Weber and White 1986, 1994; Grigg *et al.* 1993), and the α^D-globin gene has been inactivated or deleted independently in

amphibians and mammals (Hoffmann and Storz 2007; Hoffmann *et al.* 2008; Hoffmann *et al.* 2010).

Given that HbA and HbD share the same β-chain subunits, functional differences between the two isoHbs must be attributable to amino acid substitutions in the α^A- and/or α^D-globin genes. In light of what is known about the phylogenetic history of the α-like globin genes in tetrapods (Hoffmann and Storz 2007; Hoffmann et al. 2010), functional differentiation between the HbA and HbD isoforms may be attributable to post-duplication substitutions that occurred in the α^A-globin and/or α^D-globin gene lineages (Figure 1A,B,C), they could be attributable to substitutions that occurred in the single-copy, pre-duplication ancestor of the α^E- and α^D-globin genes (Figure 1D), or they could be attributable to a combination of pre- and post-duplication substitutions (Figure 1E,F). Since embryonic and adult-expressed Hbs exhibit a number of consistent functional differences (Brittain 2002), the scenarios depicted in Figure 1D,E,F suggest the possibility that HbA/D isoform differentiation may be attributable to a retained ancestral character state in HbD that harkens back to a primordial, embryonic function. To investigate this possibility and to examine the functional evolution of the α-like globin genes, in collaborative effort with the Roy E. Weber lab, Joana Projecto-Garcia, Chandrasekhar Natarajan, and Hideaki Moriyama, we conducted a combined analysis of protein biochemistry and sequence evolution to characterize the structural and functional basis of Hb isoform differentiation in birds. The main objectives were: (1) to characterize the O_2-binding properties of HbA and HbD in species that are representative of several major avian lineages; (2) to gain insight into the possible structural basis of the observed functional differentiation between the HbA and HbD isoforms; and (3) to determine whether functional differentiation between the HbA and HbD isoforms is primarily attributable to post-duplication substitutions or the retention of ancestral character states shared by HbD and embryonic Hb. Functional experiments involving purified HbA and HbD isofoms from 12 different bird species confirmed that HbD is characterized by a consistently higher O_2-affinity in the presence of allosteric effectors such as organic phosphates and Cl^- ions. Results of

the comparative sequence analysis revealed that isoHb differentiation is attributable to roughly equal numbers of post-duplication amino acid substitutions that occurred in the α^A- and α^D-globin genes.

1.2 Materials and Methods

1.2.1 Experimental Measures of Hemoglobin Function

To characterize the nature of isoHb differentiation in birds, I have collaborated with the Roy E. Weber lab and Joana Projecto-Garcia, and they performed all the experimental measurements of hemoglobin function for this study. They measured O_2-binding properties of purified HbA and HbD isoforms from a total of 12 avian species representing each of 6 orders: griffon vulture, *Gyps fulvus* (Accipitriformes: Accipitridae); greylag goose, *Anser anser* (Anseriformes: Anatidae); amazilia hummingbird, *Amazilia amazilia* (Apodiformes: Trochilidae); green-and-white hummingbird, *Amazilia viridicauda* (Apodiformes: Trochilidae); violet-throated starfrontlet, *Coeligena violifer* (Apodiformes: Trochilidae); giant hummingbird, *Patagona gigas* (Apodiformes: Trochilidae); great-billed hermit, *Phaethornis malaris* (Apodiformes: Trochilidae); common pheasant, *Phasianus colchicus* (Galliformes: Phasianidae); rook, *Corvus frugilegus* (Passeriformes: Corvidae); house wren, *Troglodytes aedon* (Passeriformes: Troglodytidae); rufous-collared sparrow, *Zonotrichia capensis* (Passeriformes: Emberizidae); and ostrich, *Struthio camelus* (Struthioformes: Struthionidae). Hbs from a disproportionate number of species were examined in Apodiformes and Passeriformes because these are the two most speciose orders of birds (together accounting of nearly half of all avian species diversity), and because both orders have been underepresented in previously published studies of avian Hb function.

Blood samples were obtained according to methods described by Weber *et al.* (1988) and Nothum *et al.* (1989). Washed red cells were frozen at -70°C, and were subsequently thawed by adding two volumes of distilled water and 1/3 volume of 1 M Tris/HCl buffer, pH 7.5. For each individual specimen, Hb isoform composition was characterized by means of alkaline polyacrylamide gel electrophoreses and/or thin-layer isoelectric focusing (PhastSystem, GE Healthcare Biosciences, Piscataway, NJ). Depending on the species, the HbA and HbD isoforms were separated by fast protein liquid chromatography (FPLC), DEAE anion-exchange chromatography, CM-Sepharose cation exchange-exchange chromatography, and/or preparative electrofocusing, as previously described (Hiebl *et al.* 1988; Weber *et al.* 2002, 2004). The separate isoHbs were further stripped of organic phosphates by passing the samples through a mixed bed resin column (MB-1 AG501-X8; BioRad, Hercules, CA) using FPLC. Hb solutions were then saturated with carbon monoxide, dialyzed at 5°C for at least 24 hr against three changes of CO-saturated 0.01 M Tris/HCl buffer, pH 7.5, containing 0.5 mM EDTA. In cases where partial oxidation (metHb formation) was evident, Hb was reduced by adding sodium dithionite, followed by dialysis against Tris buffer containing EDTA, as described by Weber *et al.* (1988). For the Hbs of the rufous-collared sparrows, house wrens, and the five hummingbird species, 10 mM HEPES as the dialysis buffer was used.

O_2-equilibrium curves for purified HbA and HbD isoforms were measured using a modified gas diffusion chamber coupled to cascaded Wösthoff pumps for mixing pure N_2 (99.998%), O_2, and atmospheric air. Changes in the absorbance spectra of thin-layer Hb solutions (4 µl) were measured in conjunction with stepwise changes in the partial pressure of O_2 (PO_2) inside the chamber. Values of P_{50} (the PO_2 at which heme is 50% saturated) and n_{50} (Hill's cooperativity coefficient at 50% saturation) were interpolated from linear plots of log [Y/(Y-1)] vs. log PO_2 for at least 4 values of Y (fractional saturation) between 0.25 and 0.75. To assess variation in the sensitivity of Hb-O_2 affinity to allosteric effectors (ligands that alter Hb-O_2 affinity by reversibly binding to sites remote from the active site), O_2-equilibrium curves of Hbs were measured by

being suspended in 0.10 M NaHEPES buffer, in the absence of added effectors ('stripped'), in the presence of inositol hexaphosphate (IHP, at IHP/Hb tetramer ratio, 2.0), in the presence of 0.10 M Cl^- ions (added as potassium chloride, KCl), and in the presence of both effectors ([Heme], 0.3 mM, unless otherwise specified). IHP is a chemical analog of inositol pentaphosphate (IPP), which is the most potent allosteric effector molecule in avian red cells (Brygier and Paul 1976; Lutz 1980).

In the case of pheasant HbA and HbD, a detailed analysis of allosteric interactions was conducted based on measurements of O_2 equilibria that included extremely high and extremely low saturation values. This allowed the Weber lab to analyze the data in terms of the two-state Monod-Wyman-Changeux (MWC) allosteric model (Monod *et al.* 1965), which relates Hb-O_2 saturation (Y) to the partial pressure of O_2 (P), the O_2 association constants for 'R-state' oxyHb and 'T-state' deoxyHb (K_R and K_T, respectively), the allosteric constant (L), and the number of interacting O_2 binding sites (q):

$$Y = \frac{LK_TP\{1 + K_TP\}^{(q-1)} + K_RP\{1 + K_RP\}^{(q-1)}}{L(1 + K_TP)^q + (1 + K_RP)^q}$$

This equation was fit to the data in the form log (Y/1-Y) *versus* log P (end-weighting) and parameters were estimated using the curve-fitting procedure described by Weber *et al.* (1995). In separate analyses, values of q were estimated from the data or were fixed at 4, as applies to tetrameric Hb. The two-state MWC parameters derived for q=4 were used to calculate the intrinsic Adair constants that characterize the affinities of 4 successive heme oxygenation steps (Adair 1925; Ferry and Green 1929):

$k_1 = (K_R + LK_T)/(1 + L)$

$k_2 = (K^2_R + LK^2_T)/(K_R + LK_T)$

$k_3 = (K^3_R + LK^3_T)/(K^2_R + LK^2_T)$

$k_4 = (K^4_R + LK^4_T)/(K^3_R + LK^3_T)$

The half-saturation value, P_{50}, was calculated as the PO_2 at log (Y/1-Y) = 0, and the median PO_2, P_m, was calculated as:

$$P_m = \left\{\frac{1}{K_R}\right\}\left[\frac{L+1}{Lc^q+1}\right]^{1/q}$$

where $c = K_T/K_R$ (Imai 1982). The maximum slope of the log-log plot, n_{max}, was calculated by first solving for PO_2 in the equation:

$$\frac{d^2\{log\left[\frac{S}{1-S}\right]\}}{d\{log(PO_2)\}^2} = 0$$

and then using that value to calculate $d(\log[Y/(1-Y)])/d(\log PO_2)$. The free energy of cooperativity, ΔG, was calculated as:

$$\Delta G = \frac{RT \ln\{(L+1)(Lc^q+1)\}}{(Lc+1)(Lc^{q-1}+1)}.$$

The O_2-binding data are not strictly comparable to those of some previously published studies because some workers measured O_2 equilibria using ionic buffers that alter the proton and anion sensitivity of Hb-O_2 affinity (Weber 1992). Nonetheless, measurements of O_2-binding properties for HbA and HbD should be internally consistent within a given study, so it is possible to compare relative levels of isoHb differentiation among studies. Thus, for the purpose of making broad-scale comparisons of isoHb differentiation among species, I surveyed published studies of

avian Hbs and compiled measures of the difference in log transformed P_{50} values between HbA and HbD in the presence and absence of IHP.

1.2.2 Molecular Modeling

In collaborative effort with Hideaki Moriyama, we built homology-based structural models of pheasant HbA and HbD isoforms using SWISS-MODEL (Arnold *et al.* 2006). For the molecular dynamics modeling, Hideaki Moriyama used deoxyhemoglobin (Proten Data Bank ID, 2HHB) as a template to maintain consistency with the results of Riccio *et al.* (2001) and Tamburrini *et al.* (2000). The root-mean square deviations between the templates and models of the α^A, α^D, and β chains were less than 0.08, 0.09, and 0.10 Å, respectively. These structures were used to calculate surface potentials using the PBEQ solver found on the CHARMM GUI server (Jo *et al.* 2008). I used the Swiss Institute of Bioinformatics ExPASy proteomics server (Gasteiger *et al.* 2003) to estimate the isoelectric point (*pI*) of the observed and reconstructed α-chain globin structures. Finally, Hideakie Moriyama conducted molecular dynamics simulations to predict O_2 and IHP binding energies using AutoDock Vina (Trott and Olson 2010). The search box for IHP (3HXN) was 25Å cubic centered on the α-chain dyad cleft, and that for O_2 (1DN2) was 5 Å cubic centered on the O_2-binding heme iron.

1.2.3 Taxon Sampling for the Molecular Evolution Analysis

The phylogenetic survey of amino acid divergence among the avian α-like globin genes included a total of 54 species, including 10 of the 12 species that were used as subjects for the experimental studies of Hb function (Table 1). In collaboration with Chandrasekhar Natarajan, he and I cloned and sequenced the α^A-, α^D-, and/or α^E-globin genes from 28 of the bird species, and the remaining sequences were retrieved from public databases. 98 homologous α-like globin

sequences from species that are representative of the other main tetrapod lineages (amphibians, nonavian reptiles, and mammals) as well as teleost fish (Table 2) were also included in the analysis.

1.2.4 Molecular Cloning and Sequencing

Genomic DNA was isolated from frozen liver tissues using the DNeasy kit and RNA was isolated from frozen whole blood or frozen pectoral muscle using the RNeasy kit (Qiagen, Valencia, CA). Chandrasekhar Natarajan and I designed paralog-specific PCR primer combinations for the α^{E}-, α^{D}-, and α^{A}-globin genes by using multispecies alignments of orthologous sequences from available avian genome assemblies (Hoffmann *et al.* 2010; Hoffmann *et al.* 2011). For each species, the α^{E}-globin gene was PCR-amplified from genomic DNA using the Invitrogen Taq Polymerase Native kit (Invitrogen, Carlsbad, CA) and the following thermal cycling protocol: 94°C (10 min) initial denaturing, (94°C [30 s], 54°C - 62.5°C [30 s] 72°C [1 min]) for 34 cycles, followed by a final extension at 72°C (7 min). The α^{D}- and α^{A}-globin genes were PCR-amplified from genomic DNA, as described above, or cDNAs were amplified from RNA using the QIAGEN OneStep RT-PCR Kit (Qiagen, Valencia, CA). Reverse transcriptase (RT) PCR reactions were conducted according to the following thermal cycling protocol: 50°C (30 min) followed by a 94°C (15 min) initial denaturing, (94°C [30 s], 55°C [30 s] 72°C [1 min]) for 34 cycles, followed by a final extension at 72°C (3 min).

For some species, Chandrasekhar Natarajan sequenced the α^{A}- and α^{D}-globin coding regions by using RACE (rapid amplification of cDNA ends). Primers were designed in the conserved exonic regions of the α^{A}- and α^{D}-globin genes and the first strand synthesis was carried out using SuperScript™ II Reverse Transcriptase (Invitrogen, Carlsbad, CA). Both 5' and 3'

RACE were performed according to the manufacturer's protocol. Sequences of all PCR, RT-PCR and RACE primers are provided in Table 3.

PCR products were electrophoretically separated on a 1.2% agarose gel (100 volts), and were then excised and eluted from the gel following the protocol in the QIAquick Gel Extraction Kit (Qiagen, Valencia, CA). PCR amplicons were cloned into pCR4-TOPO vector (Invitrogen, Carlsbad, CA), which was then used to transfect One Shot TOP10 Chemically Competent *E. coli* cells (Invitrogen, Carlsbad, CA). Positive clones were sequenced on an ABI 3730XL high-throughput capillary DNA analyzer (Applied Biosystems, Foster City, CA) using internal T7/T3 primers. All sequences were deposited in GenBank under the accession numbers: JQ405307-JQ405317, JQ405319-JQ405326, JQ697045-70, JQ405318, and JQ824132.

1.2.5 Prediction of Functionally Divergent Sites

To nominate candidate sites for functional divergence between the avian α^A- and α^D-globin sequences, residue positions were identified that were highly conserved within each paralogous clade, but which differed between the two clades. Such sites were termed 'constant-but-different' (CBD) sites by Gribaldo *et al.* (2003) and were termed 'type II' divergent sites by Gu (2001). My analysis of functional divergence was based on a total of 92 sequences (47 avian α^A-globin sequences and 45 avian α^D-globin sequences). To quantify the conservation of physicochemical properties at each residue position within the separate sets of α^A- and α^D-globin sequences, I calculated site-specific entropy values (Shannon 1948): $H_{\mathrm{i}} = -\sum_{j}^{i} p_{\mathrm{j}} \log_b p_{\mathrm{j}}$, where p_j is the frequency of a particular physicochemical state at site j, and b=8 such that calculated values fall within the interval (0, 1). In addition to considering single-residue insertions or deletions, I considered 8 possible physicochemical states for each residue position: hydrophobic (Ala, Val, Ile, Leu), hydrophilic (Ser, Thr, Asn, Gln), sulfur-containing (Met, Cys), glycine (Gly), proline

(Pro), acidic (Asp, Glu), basic (His, Lys, Arg), and aromatic (Phe, Trp, Tyr). I identified CBD sites as residue positions that were highly conserved within each set of orthologous sequences (H_i<0.5) but which exhibited a consistent physicochemical difference between the α^A- and α^D-globin sequences. CBD sites do not necessarily represent fixed amino acid differences between the α^A- and α^D-globin paralogs, since a given site could be variable for an interchangeable set of isomorphous residues within each set of orthologous sequences.

1.2.6 Ancestral Sequence Reconstruction

To infer the phylogenetic distribution of amino acid substitutions that contributed to functional differentiation between the avian HbA and HbD isoforms, I reconstructed ancestral sequences at four separate nodes in the phylogeny of α-like globin genes: (1) the single-copy proto-α globin gene in the stem lineage of tetrapod vertebrates, (2) the single-copy ancestor of the α^E- and α^D-globin paralogs in the stem lineage of tetrapods, (3) the ancestral α^D-globin in the stem lineage of birds, and (4) the ancestral α^A-globin in the stem lineage of birds. To reconstruct ancestral α-chain sequences, I applied the maximum likelihood approach of Yang *et al.* (1995) using the WAG + F model of amino acid substitution (Cao *et al.* 1994; Whelan and Goldman 2001) as implemented in PAML 4.4 (Yang 2007). Amino acid sequences were aligned using the default parameters in Muscle (Edgar 2004). The ancestral sequence reconstruction was based on a phylogeny of α-like globin sequences from a representative set of mammals, birds, nonavian reptiles, and amphibians, and the tree was rooted with α-globin sequences from teleost fishes. Ancestral states of individual sites were reconstructed independently, and I restricted the analysis to sites that had posterior probabilities ≥0.8 for a given residue or physicochemical property.

In the phylogeny of α-like globin genes, (α^A (α^D, α^E)), site-specific amino acid differences between the avian α^A- and α^D-globin sequences could be attributable to substitutions on (*i*) the branch leading to α^A, (*ii*) the post-duplication branch leading to α^D, and/or (*iii*) the pre-duplication

branch leading to the single copy ancestor of α^D and α^E (Figure 1). Accordingly, I identified all amino acid substitutions that distinguish the avian α^A- and α^D-globin paralogs and, after reconstructing ancestral states at relevant nodes of the phylogeny, I mapped the observed substitutions onto the branches mentioned above. Mapping charge-changing substitutions onto branches of the phylogeny also allowed us to reconstruct the causes of divergence in isoelectric point (*pI*) between the HbA and HbD isoforms.

1.3 Results

1.3.1 Relative Abundance of HbA and HbD

Eleven of the bird species included in this study expressed two main Hb isoforms that were clearly referable to HbA and HbD. The griffon vulture, *Gyps fulvus*, expressed three isoHbs, one of which is clearly identifiable as HbD, and the other two incorporated the products of duplicated α^A-globin genes (HbA and HbA'). The species examined generally expressed the HbA and HbD isoforms in a ~3:1 ratio, which is consistent with results from previous studies (Table 4). The pheasant represented the sole exception to this pattern, as HbD was present at a higher concentration than HbA (69% vs. 31%). HbD expression has been secondarily lost in representatives of 6 avian orders (Ciconiiformes, Columbiformes, Coraciiformes, Cuculiformes, Psittaciformes, and Sphenisciformes; Table 4), and parsimony-based character-state mapping (using the phylogeny of Hackett *et al.* 2008) suggests that each of these losses occurred independently.

1.3.2 Functional Properties of Avian HbA and HbD Isoforms

O_2-equilibrium measurements revealed consistent functional differences between the HbA and HbD isoforms, as HbD was generally characterized by a higher O_2 affinity (lower P_{50}) in the presence of IHP (two-fold molar excess over heme) and in the presence of IHP + 0.1 M Cl^- (Table 5). This pattern of isoHb differentiation is consistent with previously published results for avian Hbs (Table 6). HbD was generally characterized by a higher instrinsic O_2 affinity than HbA, but there were several exceptions. In the griffon vulture, HbD showed a much lower O_2 affinity than HbA in the absence of effectors but a higher affinity in the presence of IHP (Table 5). Likewise, in 4 of the 5 hummingbird species that Joana Project-Garcia examined (amazilia hummingbird, green-and-white hummingbird, violet-throated starfrontlet, and great-billed hermit), the HbA isoform exhibited a slightly higher intrinsic O_2 affinity than HbD. In all cases these differences in O_2 affinity were reversed in the presence of IHP (Table 5). Vandecasserie *et al.* (1973) also reported that the HbA isoforms of mallard duck, pheasant, and turkey had higher intrinsic O_2 affinities than the co-expressed HbD isoforms, and again, this was reversed in the presence of anionic effectors (Table 6). Contrary to the results reported by Vandecasserie *et al.* (1973), the O_2-equilibrium measurements on pheasant Hbs revealed a lower O_2 affinity in HbA than in co-expressed HbD in the presence *and* in the absence of anionic effectors - as found in most other species that express both isoforms (Tables 5 and 6). Whereas O_2-binding experiments from the Weber lab were carried out using zwitterionic HEPES buffer, those by Vandecasserie *et al.* (1973) were carried out using an ionic Tris-HCl buffer that may perturb the measurements of O_2 affinity by reducing the concentration of free anionic effectors in a pH-dependent manner (Weber 1992). The results from this study and those of Vandecasserie *et al.* (1973) are in agreement that the O_2 affinity of HbA is lower than that of HbD in the presence of anionic effectors, the state that is most relevant to *in vivo* conditions.

The O_2 affinities of pheasant HbA and HbD were modulated by pH in a similar fashion, as estimated Bohr factors were virtually identical for both isoHbs ($\varphi = \Delta \log P_{50}/\Delta pH$ = -0.43 at 25ºC and pH 7.0-7.5). The Bohr factor was slightly reduced at 37ºC (φ for HbA = -0.37), in

accordance with the temperature-dependence of proton dissociation, but was strongly increased in the presence IHP (φ = -0.63 at 37°C), which is consistent with the induction of basic proton binding groups by this anionic effector (Gill *et al.* 1980). When stripped of allosteric effectors, HbA and HbD exhibited similar cooperativity coefficients (n_{50} ~2.0 at 37ºC and pH 7.0 - 7.5) that increased in the presence of IHP (n_{50} ~2.6). The mixture of purified HbA and HbD isoforms exhibited P_{50} values that were intermediate to those of the individual isoHbs at physiological pH (Figure 2), which indicates the absence of functionally-significant intracellular interaction between the two isoforms. This lack of interaction, in conjunction with the observed symmetry of O_2-binding curves (reflected by the correspondence between n_{max} and n_{50} values and between P_m and P_{50} values; Table 7), justifies the quantification of the allosteric interactions of both isoforms in terms of shifts in P_{50} values (Wyman 1964).

Extended Hill plots for the HbA and HbD isoforms (Figure 3) and estimates of the MWC parameters (Table 7) elucidate the allosteric control mechanisms that underlie the observed hetero- and homotropic effects. When measured at the same pH, extended Hill plots for HbA and HbD are almost superimposed, revealing nearly identical association constants in the deoxygenated and oxygenated states (K_T and K_R, which can be interpolated from the intercepts of the lower and the upper asymptotes of the extended Hill plots with the vertical line at log PO_2 = 0; Figure 3A). Thus, both isoHbs are characterized by similar free energies of Hb cooperativity (ΔG = ~8.4 and ~8.0 for HbA and HbD, respectively, with q= free at pH ~7.5; Table 7). Whereas increased proton activity (decreased pH) decreases O_2 affinity by lowering K_T without markedly affecting K_R, IHP decreases O_2 affinity by lowering K_T more than K_R, such that both effectors raise ΔG. The effect of IHP on both K_T and K_R (Figure 3B), indicates that this effector binds to the deoxy as well as the oxy structures. Similar effects of IHP have been documented in human and fish Hbs, although physiological levels of the autochthonous phosphate effectors (DPG and ATP, respectively) primarily modulate K_T (Tyuma *et al.* 1973; Weber *et al.* 1987). As shown in

Figure 3B, increased temperature lowers K_R more than K_T, thereby decreasing the free energy of heme-heme cooperativity.

The allosteric T-state→R-state transitions of pheasant HbA and HbD and their dependence on modulating factors are further illustrated by the Adair association constants ($k_{1\text{-}4}$) for the four successive oxygenation steps. In stripped HbA and HbD at pH ~7.5, the similar k_1 and k_2 constants and the marked increases in k_3 and k_4 indicate that the allosteric transition occurs only after binding the second and third O_2 molecules (Figure 4). This also applies at lowered pH (~7.0), where lower k_1 and k_2 values show that proton binding additionally reduces the affinities for binding the 1st and 2nd O_2 molecules. In the presence of IHP, the even lower values of k_1, k_2, and k_3 combined with a drastically increased k_4 (Figure 4) indicate that IHP suppresses the affinities of unliganded hemes for the 1st, 2nd, and 3rd O_2 molecules but has little effect on the affinity of the remaining unliganded heme. This indicates that IHP-binding delays the T-state→R-state transition in quaternary structure until the final oxygenation step.

1.3.3 Insights into the Evolutionary Origins of Hb Isoform Differentiation

Comparison of avian α^A and α^D sequences yielded a Poisson-corrected amino acid divergence of 35.6%. 39 total candidate sites were identified that may contribute to functional divergence between the avian α^A- and α^D-globin genes (Figure 5), 33 of which are CBD sites (both paralogs having H_i values <0.50). The remaining 6 sites were more variable in one or both sets of orthologous sequences (Table 8). Ancestral sequence reconstructions revealed that roughly equal numbers of substitutions occurred on the post-duplication branches leading to α^A- and α^D-globin. Substitutions at 11 sites were consistent with the scenario depicted in Figure 1A, substitutions at 12 sites were consistent with Figure 1B, and substitutions at 5 sites were consistent with Figure 1C. None of the divergent sites between the α^D- and α^A-globin sequences were consistent with the scenarios depicted in Figure 1D, E, or F. The pattern was similar when considering the complete

set of 39 substitutions (including sites for which ancestral state reconstructions had posterior probabilities <0.8; Table 8). The sole exception is that the inferred history of substitution at site α9 was consistent with the scenario depicted in Figure 1D.

Charge-changing substitutions at 17 solvent-exposed residue positions account for the observed difference in net surface charge between HbA (mean pI = 8.67) and HbD (mean pI = 7.09). Substitutions at 8 sites were consistent with the scenario depicted in Figure 1A (71, 89, 90, 116, 117, 130, and 138), substitutions at 8 sites were consistent with the scenario depicted in Figure 1B (11, 30, 53, 68, 75, 82, 85, and 115), and substitutions at 2 sites were consistent with the scenario depicted in Figure 1C (8 and 15).

1.3.4 Insights into the Structural Basis of Hb Isoform Differentiation

The simulation-based autodocking experiments predicted a slightly lower O_2-binding energy (and hence, higher O_2-affinity) for the α-chain heme groups of HbD relative to those of HbA: -0.5 kcal/mol vs. -0.4 kcal/mol, respectively. The molecular dynamics simulations also predicted that the 'additional' α-chain phosphate binding site of HbD (*sensu* Tamburrini *et al.* [2000] and Riccio *et al.* [2001]) has a slightly lower IHP binding energy relative to that of HbA (Table 9), and that the bound IHP molecule is lodged more deeply in the α-chain binding cleft of HbD (Figure 6). This isoform difference in the stereochemistry of IHP binding is mainly attributable to substitutions at three symmetry-related pairs of amino acid residues: α^{D}1-Met (which reduces electrostatic repulsion relative to α^{A}1-Val), α^{D}138-Glu (which increases electrostatic attraction relative to α^{A}138-Ala), and α^{D}134-Ala (which, relative to α^{A}134-Thr, reduces steric hindrance in the cleft between the α_1 and α_2 subunits).

1.4 DISCUSSION

1.4.1 IsoHb Composition of Avian Red Cells

In contrast to the variable patterns of Hb heterogeneity in fishes and other ectothermic vertebrate groups (Binotti *et al.* 1971; Weber and Jensen 1988; Weber 1990, 1996, 2000; Ingermann 1997; Weber *et al.* 2000b), the two-component HbA/HbD system of birds is remarkably consistent. A number of bird species are known to express three or four structurally distinct isoHbs in definitive erythrocytes (Saha and Ghosh 1965; Lee *et al.* 1976; Oberthür *et al.* 1983; Hiebl *et al.* 1988; Nothum *et al.* 1989), but in all such cases, HbA and HbD (i.e., tetrameric assemblies that incorporate the products of α^A- and α^D-globin, respectively) represent the two main isoforms. HbD expression has also been secondarily lost in a number of avian taxa (e.g., pigeons, parakeets, cuckoos, jays, herons, storks, and penguins; Saha and Ghosh 1965; Vandecasserie *et al.* 1973; Godovac-Zimmermann and Braunitzer 1984, 1985; Oberthür *et al.* 1986; Sultana *et al.* 1989; Tamburrini *et al.* 1994). The same appears to be true for crocodilians (Weber and White 1986, 1994; Grigg *et al.* 1993), the sister group to Aves.

1.4.2 Structural and Functional Differentiation between HbA and HbD

It is difficult to pinpoint specific substitutions that may be responsible for isoHb differences in intrinsic O_2-affinity, although substitutions at intersubunit contact surfaces are good candidates: three of the CBD sites (114, 115, and 117) represent $\alpha_1\beta_1$ 'packing' contacts. Substitutions at intersubunit contacts often have the effect of increasing Hb-O_2 affinity by loosening constraints on the T-state quaternary structure, thereby shifting the allosteric equilibrium in favor of the high-affinity R-state (Perutz 2001). It is also possible that isoHb differences in intrinsic O_2-affinity are attributable to different combinations of substitutions in

different species. Studies of isoHb differentiation in the tufted duck, common swift, Rüppell's griffon, and goshawk suggested that the higher O_2-affinity of HbD may be attributable to the possession of α^D38-Gln or Thr instead of α^A38-Pro (Hiebl *et al.* 1987, 1988; Weber *et al.* 1988; Nothum *et al.* 1989; Abbasi and Lutfullah 2002; Lutfullah *et al.* 2005). In Hbs with α38-Gln or Thr, the R-state (oxy) structure is stabilized by two hydrogen bonds with β97-His and β99-Asp, whereas only the latter hydrogen bond is possible in the T-state. Thus, HbD with α^D38-Gln or Thr is more highly stabilized in the R-state, and the allosteric equilibrium is shifted in favor of this high-affinity quaternary structure. This structural mechanism may contribute to O_2-affinity differences between HbA and HbD in the particular species mentioned above, but it does not provide a general explanation for the observed patterns of functional differentiation between avian HbA and HbD because the majority of bird species retain the ancestral Gln residue at this intersubunit contact site in both α^A- and α^D-globin.

In addition to the isoHb differences in intrinsic O_2-affinity, HbD also exhibits a consistently higher O_2-affinity in the presence of IHP (Tables 5 and 6). This indicates that HbD is less responsive to the inhibitory effects of IHP, a potent allosteric effector that preferentially binds and stabilizes the low-affinity T-state quaternary structure of the Hb tetramer. The uniform difference in IHP sensitivity between HbA and HbD is surprising because the main polyphosphate binding site is formed by a cluster of positively charged β-chain residues that line the interior of the central cavity (Arnone and Perutz 1974; Tamburrini *et al.* 2000). Since HbA and HbD share identical β-chain subunits (and thus share the same phosphate-binding sites), the observed isoform differences in IHP sensitivity must be attributable to one or more substitutions between α^A- and α^D-globin that do not directly affect the main phosphate-binding site. Experimental evidence suggests that an additional polyphosphate binding site is formed by seven residues from each α-chain (sites 1, 95, 99, 134, 137, 138, and 141) which stabilize IHP via charge-charge interactions (Zuiderweg *et al.* 1981; Amiconi *et al.* 1985; Tamburrini *et al.* 2000; Riccio *et al.* 2001). Specifically, α99Lys and charged residues at the α-chain amino- and carboxy

termini of avian HbA and HbD are predicted to form six salt bridges with the negatively charged phosphate groups of IHP (Tamburrini *et al.* 2000; Riccio *et al.* 2001). This additional phosphate binding site is hypothesized to serve as an 'entry/leaving site' which modulates Hb-O_2 affinity by enhancing phosphate uptake and transfer to the main oxygenation-linked binding site between the β-chain subunits (Zuiderweg *et al.* 1981; Tamburrini *et al.* 2000; Riccio *et al.* 2001). Of the seven α-chain residues that comprise this additional phosphate binding site, four represent CBD sites that distinguish avian α^A- and α^D-globin sequences (1, 134, 137, and 138). The role of α1Val in this additional phosphate binding site is implicated by the fact that carbamylation of the α-chain amino-termini produces a 40% reduction in IHP affinity (Zuiderweg *et al.* 1981). However, even though HbD exhibits a consistently higher O_2-affinity than HbA in the presence of IHP (Tables 5 and 6), the molecular dynamics simulations predict that the additional phosphate binding site of HbD actually has a slightly lower IHP binding energy (and hence, higher IHP affinity) than that of HbA (Table 9). An alternative hypothesis suggested by results of the molecular dynamics simulations (Figure 6) is that IHP binding between the α_1 and α_2 subunits of HbD produces a second-order perturbation of quaternary structure that is propagated to the main phosphate binding site between the β-chain subunits.

1.4.3 Evolutionary Origins of IsoHb Differentiation in Birds

Of the many amino acid substitutions that distinguish avian HbA and HbD, ancestral sequence reconstructions indicate that roughly equal numbers of amino acid substitutions occurred on the post-duplication branches leading to α^A- and α^D-globin. Model-based calculations of electrostatic surface potentials revealed the specific substitutions that are responsible for observed differences in net surface charge between the two isoHbs, and again, roughly equal numbers of these substitutions occurred on the post-duplication branches leading to α^A- and α^D-globin. These results indicate that the observed functional differences between the HbA and HbD

isoforms are not attributable to the retention of an ancestral character state from the single-copy, pre-duplication ancestor of the α^{E}- and α^{D}-globin genes. The fact that the α^{A}- and α^{D}-globin genes have been jointly retained in the majority of sauropsid lineages over the past ~400 million years suggests that the functionally distinct HbA and HbD isoforms have evolved an important physiological division of labor in blood-O_2 transport. The O_2-affinity of HbA is more strongly modulated by allosteric effectors, suggesting that this isoform could play a more important role in regulating blood-O_2 affinity in response to transient changes in O_2 supply or demand, whereas the high-affinity HbD may make a more important contribution to blood-O_2 transport under conditions of arterial hypoxemia.

Acknowledgments

Chandrasekhar Natarajan (Lincoln) has been an incredible labmate and teacher, as he has helped me generate a number of sequence data, and he has patiently taught me how to generate my own sequence data. Hideaki Moriyama has also been an amazing mentor and collaborator as well, having guided me through the molecular modeling and graphics software, and providing the results for the molecular dynamics portion of my thesis. I would also like to thank R. W. Weber and his lab (Aarhus) and J. Projecto-Garcia for providing the functional data for hemoglobin oxygen-affinity. Anny Bang (Aarhus) and Kathy Williams (Lincoln) were of valuable assistance in the lab. I would also like to thank Z. A. Cheviron, F. G. Hoffmann, and S. D. Smith for helpful discussions, in addition to A. Abbasi, T. Kirkegaard, and G. Braunitzer for sharing unpublished data. This work was funded by grants from the National Institutes of Health/National Heart, Lung, and Blood Institute (R01 HL087216 and HL087216-S1) and the National Science Foundation (IOS-0949931). I gratefully acknowledge loans from frozen tissue collections at the Museum of Southwestern Biology, the Louisiana Museum of Natural History, and the Florida Museum of Natural History, and I also thank M. Berenbrink (U. Liverpool) and C. Witt (U. New Mexico) for sending blood samples.

References

Adair G. S., 1925 The hemoglobin system. IV. The oxygen dissociation curve of hemoglobin. J. Biol. Chem. **63**: 529-545.

Alev C., K. Shinmyozu, B. A. S. McIntyre, and G. Sheng, 2009 Genomic organization of zebra finch α- and β-globin genes and their expression in primitive and definitive blood in comparison with globins in chicken. Dev. Genes. Evol. **219**: 353-360.

Amiconi G., A. Bertollini, A. Bellelli, M. Coletta, S. G. Condò, *et al.*, 1985 Evidence for two oxygen-linked binding sites for polyanions in dromedary hemoglobin. Eur. J. Biochem. **150**: 387-393.

Arnold K., L. Bordoli, J. Kopp, and T. Schwede, 2006 The SWISS-MODEL Workspace: A web-based environment for protein structure homology modelling. Bioinformatics. **22**: 195-201.

Arnone A., and M. F. Perutz, 1974 Structure of inositol hexaphosphate--human deoxyhemoglobin complex. Nature. **249**: 34-36.

Binotti I., S. Giovenco, B. Giardini, E. Antonini, M. Brunori, *et al.,*1971 Studies on the functional properties of fish hemoglobins. II. The oxygen equilibrium of the isolated hemoglobin components from trout blood. Arch. Biochem. Biophys. **142**: 274–280.

Brittain T., 2002 Molecular aspects of embryonic hemoglobin function. Mol. Aspects Med. **23**: 293-342.

Bunn H. F., and B. G. Forget, 1986 *Hemoglobin: molecular, genetic and clinical aspects*. Saunders Co., Philadelphia.

Brygier J., and C. Paul, 1976 Oxygen equilibrium of chicken hemoglobin in the presence of organic phosphates. Biochimie. **58**: 755-756.

Cirotto C., F. Panara, and I. Arangi, 1987 The minor hemoglobins of primitive and definitive erythrocytes of the chicken embryo. Evidence for hemoglobin L. Development. 1987. **101**: 805-813.

Cao Y., J. Adachi, A. Janke, S. Pääbo, and M. Hasegawa, 1994 Phylogenetic relationships among eutherian orders estimated from inferred sequences of mitochondrial proteins: instability of a tree based on a single gene. J. Mol. Evol. **39**: 519–527.

Dickerson R. E., and I. Geis, 1983 *Hemoglobin: structure, function, evolution, and pathology*. Benjamin/Cummings Publishing, Menlo Park, CA

Edgar R. C., 2004 MUSCLE: multiple sequence alignment with high accuracy and high throughput. Nucleic Acids Res. **32**: 1792-1797.

Ferry M. F., and A. A. Green, 1929. Studies in the chemistry of hemoglobin. III. The equilibrium between oxygen and hemoglobin and its relation to changing hydrogen ion activity. J. Biol. Chem. **81**: 175-203.

Gasteiger E., A. Gattiker, C. Hoogland, I. Ivanyi, R. D. Appel, *et al.,* 2003 ExPASy: the proteomics server for in-depth protein knowledge and analysis. Nucleic Acids Res. **31**: 3784-3788.

Gill S. J., H. T. Gaud, and B. G. Barisas, 1980 Calorimetric studies of carbon monoxide and inositol hexaphosphate binding to hemoglobin A. J. Biol. Chem. **255**: 7855-7857.

Godovac-Zimmermann J., and G. Braunitzer, 1984 Hemoglobin of the adult white stork (*Ciconia ciconia*, ciconiiformes). The primary structure of α^A- and β-chains from the only present hemoglobin component. Hoppe-Seyler's Z. Physiol. Chem. **365**: 1107-1113.

Godovac-Zimmermann J., and G. Braunitzer, 1985 The primary structure of α^A- and β-chains from blue-and-yellow macaw (*Ara ararauna*, Psittaci) hemoglobin. No evidence for expression of α^D-chains. Biol. Chem. Hoppe-Seyler. **366**: 503-508.

Gorr T., 1993 Haemoglobine: Sequenz und Phylogenie. Die Primärstruktur von Globinketten des Quastenflossers (*Latimeria chalumnae*) sowie folgender Reptilien: Galapagos-Meerechse (*Amblyrhynchus cristatus*), Grüner Leguan (*Iguana iguana*), Indigonatter (*Drymarchon corais*), Glattstirnkaiman (*Paleosuchus palpebrosus*). Ph.D. Thesis, University of Munich, Germany.

Gribaldo S., D. Casane, P. Lopez, and H. Philippe, 2003 Functional divergence prediction from evolutionary analysis: A case study of vertebrate hemoglobin. Mol. Biol. Evol. **20**: 1754–1759.

Grigg G. C., R. M. G. Wells, and L. A. Beard, 1993 Allosteric control of oxygen binding by hemoglobin during development in the crocodile *Crocodylus porosus*: the role of red cell organic phosphates and carbon dioxide. J. Exp. Biol. **175**: 15-32.

Gu X., 2001 Maximum-Likelihood approach for gene family evolution under functional divergence. Mol. Biol. Evol. **18**: 453–464.

Hackett S. J., R. T. Kimball, S. Reddy, R. C. Bowie, E. L. Braun, *et al.,* 2008 A phylogenomic study of birds reveals their evolutionary history. Science. **320**: 1763-1768.

Hiebl I., J. Kösters, and G. Braunitzer, 1987 The primary structures of the major and minor hemoglobin component of adult goshawk (*Accipiter gentilis,* Accipitrinae). Biol. Chem. Hoppe-Seyler. **368**: 333-342.

Hiebl I., R. E. Weber, D. Schneeganss, and G. Braunitzer, 1989 High-altitude respiration of Falconiformes. The primary structure and functional properties of the major and minor

hemoglobin components of the adult white-headed vulture (*Trigonoceps occipitalis*, Aegypiinae). Biol. Chem. Hoppe-Seyler. **370**: 699–706.

Hiebl I., R. E. Weber, D. Schneeganss, J. Kösters, and G. Braunitzer, 1988 High-altitude respiration of birds. Structural adaptations in the major and minor hemoglobin component of adult Rüppell's griffon (*Gyps rueppellii*, Aegypiinae): a new molecular pattern for hypoxic tolerance. Biol. Chem. Hoppe-Seyler. **369**: 217–232.

Hoffmann F. G., J. C. Opazo, and J. F. Storz, 2008 Rapid rates of lineage-specific gene duplication and deletion in the α-globin gene family. Mol. Biol. Evol. **25**: 591-602.

Hoffmann F. G., J. C. Opazo, and J. F. Storz, 2011 Differential loss and retention of myoglobin, cytoglobin, and globin-E during the radiation of vertebrates. Genome Biol. Evol. **3**: 588-600.

Hoffmann F. G., and J. F. Storz, 2007 The α^{D}-globin gene originated via duplication of an embryonic α-like globin gene in the ancestor of tetrapod vertebrates. Mol. Biol. Evol. **24**: 1982-1990.

Hoffmann F. G., J. F. Storz, T. A. Gorr, and J. C. Opazo, 2010 Lineage-specific patterns of functional diversification in the α- and β-globin gene families of tetrapod vertebrates. Mol. Biol. Evol. **27**: 1126-1138.

Hofmann O., G. Carrucan, N. Robson, and T. Brittain, 1995 The chloride effect in the human embryonic hemoglobins. Biochem. J. **309**: 959-62.

Imai K., 1982 *Allosteric effects in hemoglobin*. Cambridge Univ. Press, Cambridge, UK.

Ingermann R. I., 1997 Vertebrate hemoglobins, pp. 357-408 in *Handbook of physiology*. Am. Physiol. Soc. Bethesda, MD.

Jensen F. B., 2004 Red blood cell pH, the Bohr effect, and other oxygenation-linked phenomena in blood O_2 and CO_2 transport. Acta Physiol. Scandinavica. **182**: 215–227.

Jo S., T. Kim, V. G. Iyer, and W. Im, 2008 CHARMM-GUI: A web-based graphical user interface for CHARMM. J. Comput. Chem. **29**: 1859-1865.

Lee K. S., P. C. Huang, and B. H. Cohen, 1976 Further resolution of adult chick hemoglobins by isoelectric focusing in polyacrylamide gel. Biochimica et Biophysica Acta. **427**: 178-196.

Lutfullah G., S. A. Ali, and A. Abbasi, 2005 Molecular mechanism of high altitude respiration: primary structure of a minor hemoglobin component from tufted duck (*Aythya fuligula*, Anseriformes). Biochem. Biophys. Res. Commun. **326**: 123-130.

Lutz P. L., 1980 On the oxygen affinity of bird blood. Amer. Zool. **20**: 187-198.

Monod J., J. Wyman, and J. P. Changeux, 1965 On the nature of allosteric transitions: a plausible model. J. Mol. Biol. **12**: 88-118.

Nikinmaa M., 2001 Hemoglobin function in vertebrates: evolutionary changes in cellular regulation in hypoxia. Resp. Phys. **128**: 317-329.

Nothum R., R. E. Weber, J. Kösters, D. Schneeganss, and G. Braunitzer, 1989 Amino-acid sequences and functional differentiation of hemoglobins A and D from swift (*Apus apus*, Apodiformes). Biol. Chem. Hoppe-Seyler. **370**: 1197-1207.

Oberthür W., and G. Braunitzer, 1984. Hemoglobins of the common starling (*Sturnus vulgaris*, Passeriformes). The primary structures of the α^A-, α^D- and β-chains. Hoppe-Seyler's Z. Physiol. Chem. **365**: 159-173.

Oberthür W., G. Braunitzer, R. Baumann, and P. G. Wright, 1983 Primary structures of the α- and β-chains from the major hemoglobin component of the ostrich (*Struthio camelus)* and American rhea (*Rhea americana*) (Struthioformes). Aspects of respiratory physiology and taxonomy. Hoppe-Seyler's Z. Physiol. Chem. **363**: 119–134.

Oberthür W., J. Godovac-Zimmermann, and G. Braunitzer, 1986 The expression of α^D-chains in the hemoglobin of adult ostrich (*Struthio camelus*) and American rhea (*Rhea americana*). The different evolution of adult bird α^A-, α^D- and β-chains. Biol. Chem. Hoppe-Seyler. **367**: 507-514.

Perutz M. F., 1983 Species adaptation in a protein molecule. Mol. Biol. Evol. **1**: 1–28.

Perutz, M. F., 2001 Molecular anatomy and physiology of hemoglobin, in *Disorders of hemoglobin: genetics, pathophysiology, and clinical management*, edited by M. H. Steinberg, B. G. Forget, D. R. Higgs, and R. L. Nagel. Cambridge University Press, Cambridge.

Perutz M. F., L. K. Steinrauf, A. Stockell, and A. D. Bangham, 1959 Chemical and crystallographic study of the two fractions of adult horse haemoglobin. J. Mol. Biol. **1**: 402-404.

Riccio A., M. Tamburrini, B. Giardina, and G. di Prisco, 2001 Molecular dynamics analysis of a second phosphate site in the hemoglobins of the seabird, south polar skua. Is there a site-site migratory mechanism along the central cavity? Biophys. J. **81**: 1938-1946.

Riggs A., 1976 Factors in the evolution of hemoglobin function. Fed. Proc. **35**: 2115-8.

Riggs A., 1979 Studies of the hemoglobins of Amazonian fishes-overview. Comp. Biochem. Physiol. **62A**: 257-272.

Saha A., and J. Ghosh, 1965 Comparative studies on avian hemoglobins. Comp. Biochem. Physiol. **15**: 217-235.

Sanna M. T., B. Manconi, G. Podda, A. Olianas, M. Pellegrini, M. Castagnola, I. Messana, and B. Giardina, 2007 Alkaline Bohr effect of bird hemoglobins: the case of the flamingo. Biol. Chem. **388**: 787-95.

Shannon C. E., 1948 A mathematical thheory of communication. Bell System Technical J. **27**: 379–423, 623–656.

Storz J. F., F. G. Hoffmann, and J. C. Opazo, 2011a Phylogenetic diversification of the globin gene superfamily in chordates. IUBMB Life. **63**: 313-322.

Storz J. F., F. G. Hoffmann, J. C. Opazo, T. J. Sanger, and H. Moriyama. 2011b Developmental regulation of hemoglobin synthesis in the green anole lizard, *Anolis carolinensis*. J. Exp. Biol. **214**: 575-581.

Sultana C., A. Abbasi, and Z. H. Zaidi, 1989 Primary structure of hemoglobin α-chain of *Columba livia* (gray wild pigeon). J. Protein Chem. **8**: 629-646.

Takei H., Y. Ota, K. Wu, T. Kiyohara, and G. Matsuda, 1975 Amino acid sequence of the α-chain of chicken AI hemoglobin. J. Biochem. **77**: 1345-1347.

Tamburrini M., S. G. Condò, G. di Prisco, and B. Giardina, 1994 Adaptation to extreme environments: structure-function relationships in emperor penguin hemoglobin. J. Mol. Biol. **237**: 615-621.

Tamburrini M., A. Riccio, M. Romano, B. Giardina, and G. Prisco, 2000 Structural and functional analysis of the two hemoglobins of the Antarctic seabird *Catharacta maccormicki*: Characterization of an additional phosphate binding site by molecular modelling. Eur. J. Biochem. **267**: 6089-6098.

Trott O., and A. J. Olson, 2010 AutoDock Vina: improving the speed and accuracy of docking with a new scoring function, efficient optimization and multithreading. J. Comput. Chem. **31**: 455-461.

Tyuma I., K. Imai, and K. Shimizu, 1973 Analysis of oxygen equilibrium of hemoglobin and control mechanism of organic phosphates. **12**: 1491-1498.

Weber R. E., 1990 Functional significance and structural basis of multiple hemoglobins with special reference to ectothermic vertebrates, pp. 58-75, in *Animal nutrition and transport processes. 2. Transport, respiration and excretion: Comparative and environmental aspects* edited by J. P. Truchot, and B. Lahlou. Basel, Karger.

Weber, R. E., 1992 Use of ionic and zwitterionic (Tris/BisTris and HEPES) buffers in studies on hemoglobin function. J. Appl. Physiol. **72**: 1611-1615.

Weber, R. E., 1995 Hemoglobin adaptations to hypoxia and altitude—the phylogenetic perspective, pp. 31-44 in *Hypoxia and the brain: Proceedings of the 9th international hypoxia symposium*, edited by J. R. Sutton, C. S. Houston, and G. Coates. Queen City Printers, Burlington, VT.

Weber R. E., 1996 Hemoglobin adaptations in Amazonian and temperate fish with special reference to hypoxia, allosteric effectors and functional heterogeneity, pp. 75-90 in *Physiology and biochemistry of the fishes of the Amazon*, edited by A. L. Val, V. M. F. Almeida-Val, and D. J. Randall. INPA, Brazil.

Weber, R. E., 2000a Hemoglobin function in vertebrates: Molecular adaptation in extreme and temperate environments, pp. 23-37 in *Adaptations for oxygen transport: lessons from fish hemoglobins*, edited by G. Di Prisco, B. Giardina, and R. E. Weber. Springer, New York.

Weber, R. E., and A. Fago, 2004 Functional adaptation and its molecular basis in vertebrate hemoglobins, neuroglobins and cytoglobins. Respir. Physiol. Neurobiol. **144**: 141-159.

Weber, R. E., A. Fago, A. L. Val, A. Bang, M. L. van Hauwert, and S. DeWilde, *et al.,* 2000b Isohemoglobin differentiation in the bimodal-breathing Amazon catfish *Hoplosternum littorale* . J. Biol. Chem. **275**: 17297-17305.

Weber, R. E., I. Hiebl, and G. Braunitzer, 1988 High altitude and hemoglobin function in the vultures *Gyps rueppellii* and *Aegypius monachus*. Biol. Chem. Hoppe-Seyler. **369**: 233-240.

Weber, R. E., and F. B. Jensen, 1988 Functional adaptations in hemoglobins from ectothermic vertebrates. Ann. Rev. Physiol. **50**: 161-179.

Weber, R. E., H. Malte, E. H. Braswell, R. W. Oliver, B. N. Green, *et al.*, 1995 Mass spectrometric composition, molecular mass and oxygen binding of *Macrobdella decora* hemoglobin and its tetramer and monomer subunits. J. Mol. Biol. **251**: 703-20.

Weber, R. E., W. Voelter, A. Fago, H. Echner, E. Campanella, *et al.*, 2004 Modulation of red cell glycolysis: interactions between vertebrate hemoglobins and cytoplasmic domains of band 3 red cell membrane proteins. Am. J. Physiol. Regul. Integr. Comp. Physiol. **287**: R454-464.

Weber, R. E., and F. N. White, 1986 Oxygen binding in alligator blood related to temperature, diving, and "alkaline tide". Am. J. Physiol. **251**: R901-908.

Weber, R. E., and F. N. White, 1994 Chloride-dependent organic phosphate sensitivity of the oxygenation reaction in crocodilian hemoglobins. J. Exp. Biol. **192**: 1-11.

Whelan, S., and N. Goldman, 2001 A general empirical model of protein evolution derived from multiple protein families using a maximum-likelihood approach. Mol. Biol. Evol. **18**: 691-699.

Wyman, J., 1964 Linked functions and reciprocal effects in hemoglobin: a second look. Adv. Protein Chem. **19**: 223-286.

Yang, Z., 2007 PAML 4: Phylogenetic analysis by maximum likelihood. Mol. Biol. Evol. **24**: 1586-1591.

Yang, Z., S. Kumar, and M. Nei. 1995 A new method of inference of ancestral nucleotide and amino acid sequences. Genetics **141**: 1641–1650.

Vandecasserie, C., C. Paul, A. G. Schnek, and J. Leonis, 1973 Oxygen affinity of avian hemoglobins. Comp. Biochem. Physiol. A . **44**: 711–718.

Zuiderweg, E. R., L. F. Hamers, H. S. Rollema, S. H. de Bruin, and C. W. Hilbers, 1981 31^P NMR study of the kinetics of binding of myo-inositol hexakisphosphate to human hemoglobin. Observation of fast-exchange kinetics in high-affinity systems. Eur. J. Biochem. **118**: 95-104.

Appendix A.

Table 1. Accession numbers for avian α-like globin sequences.

Order	Family	Species	Accession number
Accipitriformes	Accipitridae	Northern goshawk, *Accipiter gentilis*	P08850.2, P08849.1
Accipitriformes	Accipitridae	Black vulture, *Aegypius monachus*	P07417.2, P68059.1
Accipitriformes	Accipitridae	Rüppell's griffon, *Gyps rueppellii*	P08256.1, P08257.1
Accipitriformes	Accipitridae	White-headed vulture, *Trigonoceps occipitalis*	P19832.1, P68060.1
Anseriformes	Anatidae	Mallard duck, *Anas platyrhynchos*	P01988.2, P04442.1, K01942.1
Anseriformes	Anatidae	Graylag goose, *Anser anser*	P01989.2, P04238.1
Anseriformes	Anatidae	Bar-headed goose, *Anser indicus*	P01990.2, P04239.1
Anseriformes	Anatidae	Tufted duck, *Aythya fuligula*	P84790.2, P84791.1
Anseriformes	Anatidae	Canada goose, *Branta canadensis*	ACT80863.1, P04240.1
Anseriformes	Anatidae	Muscovy duck, *Cairina moschata*	P01987.2, P02003.1, P04243.2
Anseriformes	Anatidae	Andean goose, *Chloephaga melanoptera*	ACT80387.1, P07035.1
Apodiformes	Apodidae	Common swift, *Apus apus*	P15162.2, P15164.1
Apodiformes	Trochilidae	Speckled hummingbird, *Adelomyia melanogenys*	JQ697045, JQ697061
Apodiformes	Trochilidae	White-tufted sunbeam, *Aglaeactis castelnaudii*	JQ697046, JQ697062
Apodiformes	Trochilidae	Amazilia hummingbird, *Amazilia amazilia*	JQ697047, JQ697063
Apodiformes	Trochilidae	Green-and-white hummingbird, *Amazilia viridicauda*	JQ697048, JQ697064
Apodiformes	Trochilidae	Bronzy inca, *Coeligena coeligena*	JQ697049, JQ697065
Apodiformes	Trochilidae	Violet-throated starfrontlet, *Coeligena violifer*	JQ697050, JQ697066
Apodiformes	Trochilidae	Andean hillstar, *Oreotrochilus estella*	JQ697051, JQ405318
Apodiformes	Trochilidae	Black-breasted hillstar, *Oreotrochilus melanogaster*	JQ697052, JQ697067
Apodiformes	Trochilidae	Giant hummingbird, *Patagona gigas*	JQ697054, JQ697060
Apodiformes	Trochilidae	Great-billed hermit, *Phaethornis malaris*	JQ697053 , JQ697059
Charadriiformes	Stercorariidae	South polar skua, *Catharacta maccormicki*	P82111.1, P82112.1

Columbiformes	Columbidae	Rock pigeon, *Columba livia*	P21871.2, O12985.1, JQ405311
Cuculiformes	Cuculidae	Common cuckoo, *Cuculus canorus*	BAC57968, BAC57969.1
Falconiformes	Falconidae	Prairie falcon, *Falco mexicanus*	JQ405314
Galliformes	Phasianidae	Japanese quail, *Coturnix japonica*	P24589.2, P30892.1
Galliformes	Phasianidae	Chicken, *Gallus gallus*	NP_001004376, NP_001004375.1, NP_001004374.1
Galliformes	Phasianidae	Wild turkey, *Meleagris gallopavo*	P81023.2, P81024.1, XP_003210789.1
Galliformes	Phasianidae	Common pheasant, *Phasianus colchicus*	P01995.1, P02002.1
Gruiformes	Gruidae	Sandhill crane, *Grus canadensis*	JQ405312
Opisthocomiformes	Opisthocomidae	Hoatzin, *Opisthocomus hoazin*	JQ405310
Passeriformes	Corvidae	Hooded crow, *Corvus cornix*	JQ697055, JQ405319
Passeriformes	Emberizidae	Rufous-collared sparrow, *Zonotrichia capensis*	JQ405316, JQ405315
Passeriformes	Estrildidae	Zebra finch, *Taeniopygia guttata*	XP_002196132.1, XP_002196147.1, NP_001191174.1
Passeriformes	Furnariidae	Wren-like rushbird, *Phleocryptes melanops*	JQ405307, JQ405317
Passeriformes	Passeridae	Tree sparrow, *Passer montanus*	P07407.1, P07413.1, JQ405308
Passeriformes	Sturnidae	Yellow-faced myna, *Mino dumontii*	JQ697056, JQ697069
Passeriformes	Sturnidae	Common starling, *Sturnus vulgaris*	P01997.1, P02004.1, JQ405313
Passeriformes	Troglodytidae	House wren, *Troglodytes aedon*	JQ405324, JQ697068
Passeriformes	Turdidae	Common blackbird, *Turdus merula*	P14522.1, P14523.1
Pelecaniformes	Pelecanidae	Dalmatian pelican, *Pelecanus crispus*	JQ405326, JQ405322
Pelecaniformes	Pelecanidae	Great white pelican, *Pelecanus onocrotalus*	JQ405325, JQ824132
Pelecaniformes	Phalacrocoracidae	Great cormorant, *Phalacrocorax carbo*	P10780.1, P10781.1, JQ405309
Phoenicopteriformes	Phoenicopteridae	Greater flamingo, *Phoenicopterus roseus*	JQ697057, JQ697070
Phoenicopteriformes	Phoenicopteridae	American flamingo, *Phoenicopterus ruber*	P01984.2, JQ405321
Psittaciformes	Psittacidae	Budgerigar, *Melopsittacus undulatus*	JQ697058
Psittaciformes	Psittacidae	Rose-ringed parakeet, *Psittacula krameri*	P19831.1
Strigiformes	Strigidae	Eurasian eagle owl, *Bubo bubo*	JQ405323, JQ405320

Struthioniformes	Rheidae	Greater rhea, *Rhea americana*	P01982.1, P04241.1
Struthioformes	Struthionidae	Ostrich, *Struthio camelus*	P01981.1, P04242.1

Table 2. Accession numbers for α-like globin sequences from nonavian vertebrates.

Class	Order	Family	Species	Accession number
Actinopterygii	Beloniformes	Adrianichthyidae	Japanese medaka, *Oryzias latipes*	BAC20295.1, BAC06482.1
Actinopterygii	Characiformes	Characidae	Red-tailed brycon, *Brycon cephalus*	ABL89191.1
Actinopterygii	Cypriniformes	Cyprinidae	Common carp, *Cyprinus carpio*	BAB79237.1
Actinopterygii	Cypriniformes	Cyprinidae	Zebrafish, *Danio rerio*	NP_891985.1
Actinopterygii	Esociformes	Esocidae	Northern pike, *Esox lucius*	ACO13595.1
Actinopterygii	Gadiformes	Gadidae	Polar cod, *Boreogadus saida*	Q1AGS9.3
Actinopterygii	Gadiformes	Gadidae	Atlantic cod, *Gadus morhua*	ABV21551.1
Actinopterygii	Osmeriformes	Osmeridae	Rainbow smelt, *Osmerus mordax*	ACO08865.1
Actinopterygii	Perciformes	Osmeridae	Antartic fish, *Pogonophryne scotti*	P0C238.2
Actinopterygii	Perciformes	Osmeridae	Yellow perch, *Perca flavescens*	1XQ5_A
Actinopterygii	Pleuronectiformes	Osmeridae	Turbot, *Scophthalmus maximus*	ABJ98630.1
Actinopterygii	Salmoniformes	Osmeridae	Rainbow trout, *Oncorhynchus mykiss*	ACO08763.1
Actinopterygii	Salmoniformes	Osmeridae	Atlantic salmon, *Salmo salar*	CAA65949.1
Actinopterygii	Scorpaeniformes	Osmeridae	Sablefish, *Anoplopoma fimbria*	ACQ58238.1
Actinopterygii	Scorpaeniformes	Osmeridae	Kelp snailfish, *Liparis tunicatus*	P85081.1
Actinopterygii	Siluriformes	Osmeridae	Channel catfish, *Ictalurus punctatus*	NP_001188201.1
Actinopterygii	Tetraodontiformes	Osmeridae	Fugu rubripes, *Takifugu rubripes*	AAO61492.1
Actinopterygii	Tetraodontiformes	Osmeridae	Pufferfish, *Tetraodon nigroviridis*	CAG12202.1
Amphibia	Anura	Pipidae	African clawed frog, *Xenopus laevis*	P02012.2, NP_001081493.1, P06636.2, NP_001079749.1, NP_001079746.1
Amphibia	Anura	Pipidae	Western clawed frog, *Xenopus tropicalis*	NP_988860.1, NP_001005092.1, NP_001135724.1, NP_001165373.1, NP_001107321.1, NP_001165374.1,

Amphibia	Anura	Ranidae	Bullfrog, *Rana catesbeiana*	NP_001015904.1, NP_001016009.1 P51465.2, ACO51559.1, P55267.2
Amphibia	Caudata	Ambystomatidae	Axolotl, *Ambystoma mexicanum*	P02015.2, AAK58843.1, BAD30048.1, BAD30049.1
Amphibia	Caudata	Salamandridae	Iberian ribbed newt, *Pleurodeles waltl*	P06639.4, P11896.1
Amphibia	Caudata	Salamandridae	Rough-skinned newt, *Taricha granulosa*	P02014.1, P10783.1
Mammalia	Carnivora	Canidae	Dog, *Canis lupus*	P60529.1
Mammalia	Carnivora	Felidae	Domestic cat, *Felis catus*	P07405.1
Mammalia	Carnivora	Ursidae	Giant panda, *Ailuropoda melanoleuca*	XP_002920201.1, XP_002920198.1
Mammalia	Cetacea	Delphinidae	Saddleback dolphin, *Delphinus delphis*	ACN44165.1
Mammalia	Cetacea	Delphinidae	Bottlenosed dolphin, *Tursiops truncatus*	P18978.1
Mammalia	Cetacea	Physeteridae	Sperm whale, *Physeter catodon*	P09904.1
Mammalia	Cetartiodactyla	Bovidae	Cattle, *Bos taurus*	NP_001070890.2, XP_001788743.1, XP_580707.3
Mammalia	Cetartiodactyla	Bovidae	Goat, *Capra hircus*	ACH86006.1, P13786.2
Mammalia	Cetartiodactyla	Suidae	Pig, *Sus scrofa*	XP_003481132.1, P02009.1
Mammalia	Chiroptera	Molossidae	Wrinkle-lipped free-tailed bat, *Chaerephon plicatus*	ACE60603.1
Mammalia	Chiroptera	Pteropodidae	Leschenault's rousette, *Rousettus leschenaultii*	ACE60609.1
Mammalia	Chiroptera	Phyllostomidae	California leaf-nosed bat, *Macrotus californicus*	P09839.1
Mammalia	Cingulata	Dasypodidae	Nine-banded armadillo, *Dasypus novemcinctus*	P01964.1, ACO83100.1
Mammalia	Didelphimorphia	Didelphidae	Gray short-tailed opossum, *Monodelphis domestica*	NP_001028158.1, XP_003341721.1
Mammalia	Diprotodontia	Macropodidae	Tammar wallaby, *Macropus eugenii*	P81043.3, AAX18654.1, AAX18653.1
Mammalia	Insectivora	Erinaceidae	Western European hedgehog, *Erinaceus europaeus*	P01949.1
Mammalia	Insectivora	Soricidae	European shrew, *Sorex araneus*	ACE73634.1, ACE73631.1
Mammalia	Insectivora	Talpidae	Coast mole, *Scapanus orarius*	ADJ17347.1

Mammalia	Insectivora	Talpidae	European mole, *Talpa europaea*	P01951.1
Mammalia	Lagomorpha	Leporidae	European hare, *Lepus europaeus*	3LQD_A
Mammalia	Lagomorpha	Leporidae	Rabbit, *Oryctolagus cuniculus*	NP_001075858.1, NP_001164886.1
Mammalia	Lagomorpha	Ochotonidae	Black-lipped pika, *Ochotona curzoniae*	ABO27190.1
Mammalia	Monotremata	Ornithorhynchidae	Platypus, *Ornithorhynchus anatinus*	XP_001517140.2, XP_001510395.1
Mammalia	Perissodactyla	Equidae	Horse, *Equus caballus*	P01958.2, NP_001108014.1
Mammalia	Perissodactyla	Rhinocerotidae	White rhinoceros, *Ceratotherium simum*	P01963.2
Mammalia	Perissodactyla	Tapiridae	Brazilian tapir, *Tapirus terrestris*	P01962.1
Mammalia	Primates	Hominidae	Human, *Homo sapiens*	NP_000508.1, NP_005323.1
Mammalia	Primates	Atelidae	Black-handed spider monkey, *Ateles geoffroyi*	P67817.2
Mammalia	Primates	Cebidae	White-tufted-ear marmoset, *Callithrix jacchus*	XP_002755769.1, ABZ80335.1
Mammalia	Proboscidea	Elephantidae	Asiatic elephant, *Elephas maximus*	ACV41393.1
Mammalia	Proboscidea	Elephantidae	African savanna elephant, *Loxodonta africana*	XP_003417852.1, XP_003417854.1
Mammalia	Rodentia	Cricetidae	Chinese hamster, *Cricetulus griseus*	XP_003501524.1, XP_003511891.1
Mammalia	Rodentia	Cricetidae	Deer mouse, *Peromyscus maniculatus*	ABN71059.1, ABN71228.1
Mammalia	Rodentia	Muridae	Norway rat, *Rattus norvegicus*	NP_001013875.1, NP_001166316.1
Reptilia	Crocodylia	Crocodylidae	Nile crocodile, *Crocodylus niloticus*	P01998.1
Reptilia	Crocodylia	Crocodylidae	American alligator, *Alligator mississippiensis*	P01999.2
Reptilia	Crocodylia	Crocodylidae	Spectacled caiman, *Caiman crocodilus*	0901255A, P02000.1
Reptilia	Sphenodontia	Sphenodontidae	Tuatara, *Sphenodon punctatus*	P10059.1, P10062.1
Reptilia	Squamata	Colubridae	Texas indigo snake, *Drymarchon corais*	P0C0U6.1, P0C0U7.1
Reptilia	Squamata	Iguanidae	Marine iguana, *Amblyrhynchus cristatus*	Gorr (1993)
Reptilia	Squamata	Iguanidae	Green anole, *Anolis carolinensis*	Hoffman *et al.* (2008)
Reptilia	Testudines	Cheloniidae	Loggerhead turtle, *Caretta caretta*	Q10732.1

Reptilia	Testudines	Emydidae	Western painted turtle, *Chrysemys picta*	P13273.1, P02005.1
Reptilia	Testudines	Emydidae	Red-eared slider turtle, *Trachemys scripta*	FG341498.1
Reptilia	Testudines	Testudinidae	Brazilian giant tortoise, *Geochelone denticulata*	AAM18964.1
Reptilia	Testudines	Testudinidae	Galápagos giant tortoise, *Geochelone nigra*	P83135.2
Reptilia	Testudines	Chelidae	Snake-necked turtle, *Phrynops hilarii*	P02006.1

Table 3. PCR, RT-PCR, and RACE primer sequences.

α^A-globin
HBA2.-14.F 5' - GGRCACCCGTGCTGGGGCTG - 3' and HBA2.724.R 5' - TAACGGTACTTGGCRGTCAG - 3'
HBA1.-88.ZF.F 5' - GTGATAAGATAAGGCTGGGAGG - 3' and HBA1.970.R 5' - GACACGTTGCTGCAGCAA - 3'
HBAEX1F 5' - ATGGTGCTGTCYGCKGCTGACAAGA - 3 and HBAEX3R 5' - AACGGTACTTGGCRGTCAGCAC - 3'[a]
HBAEX2F 5' - AAGTGGGGGAAGTAGGTCTTGGT - 3' and HBAEX2R 5' - ACCAAGACCTACTTCCCCCACTT - 3'[a]
AAP 5' - GGCCACGCGTCGACTAGTACGGGIIGGGIIGGGIIG - 3'[a]
UAP 5' - CUACUACUACUAGGCCACGCGTCGACTAGTAC - 3'[a]
AUAP 5' - GGCCACGCGTCGACTAGTAC - 3'[a]
5AP 5' - CUACUACUACUAGGCCACGCGTCGACTAGTACGGGIIGGGIIGGGIIG - 3'[a]
3AP 5' - GGCCACGCGTCGACTAGTACTTTTTTTTTTTTTTTT - 3'[a]
α^D-globin
PPHADF5' 5' - AACACGCAGGTTGTAGGC - 3'[a]
PPHADR3' 5' - CCAAGACCTACTTCCCCCACTTC - 3'[a]
NPHAD5' 5' - GAAGTGGGGGAAGTAGGTCTTGGTC - 3'[a]
NPHAD3' 5' - AACCTGCGTGTTGACCCCG - 3'[a]
NP2HAD5' 5' - CTTCTTGTCSTCGGCRGTCAGCAT - 3'[a]
HADEX1F 5' - ATGCTGACYGCCGASGACAAGAAG - 3' and HADEX3R 5' - ATCTGTACTTYTCAGCCAGCAC - 3'[a]
α^E-globin
Hbe_3_F 5' - GGAGTGACCAATGAGTGTGGACAG - 3' and Hbe_3_R 5' - GAAAGCACAGAGACCATAG - 3'
Hbe_4_F 5' - ACAACCTGCTCTGGGTGTTC - 3' and Hbe_4_R 5' - CCCTTTGGAGAAGAGCACAT - 3'

[a]RACE primers.

Table 4. Relative concentrations of the two primary isoHbs (HbA and HbD) in the definitive erythrocytes of adult birds.

Order	Species	HbA%	HbD%	Reference
Accipitriformes	Northern goshawk, *Accipiter gentilis*	80	20	Hiebl et al. (1987b)
Accipitriformes	Black vulture, *Aegypius monachus*	81	19	Hiebl et al. (1987c)
Accipitriformes	Golden eagle, *Aquila chrysaetos*	65	35	Oberthür et al. (1983b)
Accipitriformes	Griffon vulture, *Gyps fulvus*	66	34	Present study[a]
Accipitriformes	Rüppell's griffon, *Gyps ruppellii*	73	27	Hiebl et al. (1988)
Accipitriformes	Kite, *Milvus migrans*	70	30	Saha and Ghosh (1965)
Accipitriformes	White vulture, *Trigonoceps occipitalis*	70	30	Hiebl et al. (1989)
Anseriformes	Mallard duck, *Anas platyrhinchos*	62	38	Saha and Ghosh (1965)
Anseriformes	Greylag goose, *Anser anser*	90	10	Hiebl et al. (1986)
		92	8	Present study
Anseriformes	Bar-headed goose, *Anser indicus*	88	12	Hiebl et al. (1986)
Anseriformes	Common pochard, *Aythya ferina*	78	21	Saha and Ghosh (1965)
Anseriformes	Tufted duck, *Aythya fuligula*	90	10	Lutfullah et al. (2005)
Anseriformes	Canada goose, *Branta canadensis*	89	11	Hiebl et al. (1986)
Anseriformes	Andean goose, *Chloephaga melanoptera*	78	22	Hiebl et al. (1987a)
Apodiformes	Common swift, *Apus apus*	86	14	Nothum et al. (1989b)
Apodiformes	Amazilia hummingbird, *Amazilia amazilia*	70	30	Present study
Apodiformes	Green-and-white hummingbird, *Amazilia viridicauda*	78	22	Present study
Apodiformes	Violet-throated starfrontlet, *Coeligena violifer*	81	19	Present study
Apodiformes	Giant hummingbird, *Patagona gigas*	81	19	Present study
Apodiformes	Great-billed hermit, *Phaethornis malaris*	61	39	Present study
Charadriiformes	South polar skua, *Catharacta maccormicki*	65	35	Tamburrini et al. (2000)
Ciconiiformes	Grey heron, *Ardea cinerea*	100	0	Oberthür et al. (1986)
Ciconiiformes	Cattle egret, *Bubulcus ibis*	100	0	Saha and Ghosh (1965)

Ciconiiformes	White stork, *Ciconia ciconia*	100	0	Godovac and Braunitzer (1984)
Columbiformes	Rock pigeon, *Columba livia*	100	0	Sultana (1989)
Columbiformes	Spotted dove, *Streptopelia chinensis*	100	0	Saha and Ghosh (1965)
Columbiformes	Rufous turtle dove, *Streptopelia orientalis*	100	0	Saha and Ghosh (1965)
Columbiformes	Bengal green pigeon, *Terron phoenicoptera*	100	0	Saha and Ghosh (1965)
Coraciiformes	Bluejay, *Coracias benghalensis*	100	0	Saha and Ghosh (1965)
Cuculiformes	Greater coucal, *Centropus sinensis*	100	0	Saha and Ghosh (1965)
Cuculiformes	Indian cuckoo, *Cuculus micropterus*	100	0	Saha and Ghosh (1965)
Cuculiformes	Hawk cuckoo, *Cuculus varius*	100	0	Saha and Ghosh (1965)
Cuculiformes	Asian koel, *Eudynamys scolopacea*	100	0	Saha and Ghosh (1965)
Cathartiformes	Andean condor, *Vultur gryphus*	83	17	Bauer et al. (1985)
Galliformes	Gray quail, *Coturnix coturnis*	76	24	Saha and Ghosh (1965)
Galliformes	Grey partridge, *Francolinus pondacerianus*	75	25	Abbasi and Zaidi (1989)
Galliformes	Chicken, *Gallus gallus*	70	30	Saha and Ghosh (1965)
		71	29	Present study
		75	25	Weber et al. (2004)
Galliformes	Wild turkey, *Meleagris gallopavo*	~75	~25	Vandecasserie et al. (1973)
Galliformes	Guinea fowl, *Numida meleagris*	63	37	Saha and Ghosh (1965)
Galliformes	Pheasant, *Phasianus colchicus*	~75	~25	Braunitzer et al. (1982)
		31	69	Present study
Passeriformes	Common myna, *Aeridotheres tristis*	62	38	Saha and Ghosh (1965)
Passeriformes	Yellow eyed babbler, *Chrysomma sinensis*	68	33	Saha and Ghosh (1965)
Passeriformes	Magpie robin, *Copsychus saularis*	58	42	Saha and Ghosh (1965)
Passeriformes	Black drongo, *Dicrurus macrocercus*	63	36	Saha and Ghosh (1965)
Passeriformes	Hill myna, *Gracula religiosa*	69	31	Saha and Ghosh (1965)
Passeriformes	White throated munia, *Lonchura malabarica*	71	30	Saha and Ghosh (1965)
Passeriformes	Black headed munia, *Lonchura malacca*	69	29	Saha and Ghosh (1965)

Passeriformes	Spotted munia, *Lonchura punctulata*	71	29	Saha and Ghosh (1965)
Passeriformes	House sparrow, *Passer domesticus*	72	28	Saha and Ghosh (1965)
Passeriformes	Eurasian tree sparrow, *Passer montanus*	85	15	Schneeganss et al. (1985)
Passeriformes	Red vented bulbul, *Pycnonotus cafer*	76	24	Saha and Ghosh (1965)
Passeriformes	Red whiskered bulbul, *Pycnonotus jocosus*	70	30	Saha and Ghosh (1965)
Passeriformes	Hodgson's bush-chat, *Saxicola insignis*	70	31	Saha and Ghosh (1965)
Passeriformes	Common starling, *Sturnus vulgaris*	60	40	Oberthür et al. (1984)
Passeriformes	Common blackbird, *Turdus merula*	80	20	Nothum et al. (1989a)
Passeriformes	House wren, *Troglodytes aedon*	58	42	Present study
Passeriformes	Rufous-collared sparrow, *Zonotrichia capensis*	62	38	Present study
Pelecaniformes	Great cormorant, *Phalacrocorax carbo*	87	17	Huber et al. (1988)
Phoenicopteriformes	Greater flamingo, *Phoenicopterus roseus*	75	25	Sanna et al. (2007)
Phoenicopteriformes	American flamingo, *Phoenicopterus ruber*	75	25	Godovac and Braunitzer (1984)
Piciformes	Blue throated barbet, *Megalaima asiatica*	88	13	Saha and Ghosh (1965)
Piciformes	Lineated barbet, *Megalaima lineata*	83	17	Saha and Ghosh (1965)
Psittaciformes	Blue and yellow macaw, *Ara ararauna*	100	0	Godovac and Braunitzer (1985)
Psittaciformes	Blossom headed parakeet, *Psittacula cyanocephala*	100	0	Saha and Ghosh (1965)
Psittaciformes	Rose ringed parakeet, *Psittacula krameri*	100	0	Saha and Ghosh (1965)
Sphenisciformes	Emperor penguin, *Aptenodytes forsteri*	100	0	Tamburrini et al. (1994)
Struthioniformes	Greater rhea, *Rhea americana*	60	40	Oberthür et al. (1983a)
Struthioniformes	Ostrich, *Struthio camelus*	70	30	Oberthür et al. (1983a)
		74	23	Isaacks et al. (1980)
		79	21	Present study[b]

[a]Abbasi A, Weber RE, Braunitzer G, unpublished data

[b]Kirkegaard T, Weber RE, unpublished data

Table 5.O_2 affinities (P_{50}, torr) and cooperativity coefficients (n_{50}) of purified HbA and HbD isoforms from 12 bird species.O_2 equilibria were measured in 0.1 mM HEPES buffer at pH 7.4 (± 0.01) and 37ºC in the absence (stripped) and presence of allosteric effectors ([Cl^-], 0.1 M; [HEPES], 0.1 M; IHP/Hb tetramer ratio, 2.0. P_{50} and n_{50}values were derived from single O_2 equilibrium curves, where each value was interpolated from linear Hill plots (correlation coefficient r> 0.995) based on 4 or more equilibrium steps between 25 and 75 % saturation.

Species	IsoHb	[heme], mM	Stripped		+ KCl		+ IHP		+ KCl + IHP	
			P_{50}	n_{50}	P_{50}	n_{50}	P_{50}	n_{50}	P_{50}	n_{50}
ACCIPITRIFORMES										
Gyps fulvus	HbA	0.30			6.46	1.62			28.84	1.98
	HbD	0.07			15.86	1.82			26.61	1.99
ANSERIFORMES										
Anser anser	HbA	1.00			4.78	2.51			43.95[a]	3.00[a]
	HbD	0.72			3.59	1.90			29.79[a]	2.51[a]
APODIFORMES										
Amazilia amazilia	HbA	0.30	3.14	1.38	5.28	1.90	36.77	2.16	29.84	2.42
	HbD	0.30	3.36	1.70	4.79	2.08	28.61	2.63	23.20	2.40
Amazilia viridicauda	HbA	0.30	2.62	1.43	4.47	1.81	28.49	2.13	24.24	2.07
	HbD	0.30	2.78	1.34	3.90	1.64	21.83	2.22	20.36	2.29
Coeligena violifer	HbA	0.30	2.12	1.29	3.74	1.65	23.55	1.96	19.12	1.70
	HbD	0.30	2.48	1.40	3.65	1.80	17.70	2.30	17.01	2.46
Patagona gigas	HbA	0.30	2.52	1.46	4.14	1.63	29.97	2.28	25.86	2.49
	HbD	0.30	2.45	1.41	3.19	1.97	17.44	2.24	16.56	2.56
Phaethornis malaris	HbA	0.30	2.83	1.39	4.70	1.83	37.00	2.27	28.13	2.04
	HbD	0.30	3.06	1.62	5.02	2.11	26.03	2.47	24.92	2.72
GALLIFORMES										
Phasianus colchicus	HbA	0.08			5.62	1.86			44.67[a]	2.31[a]
	HbD	0.11			5.54	1.73				
	HbA	0.60			4.12[b]	2.47[b]			29.51[b]	2.55[b]
	HbD	0.60			3.50[b]	2.38[b]			24.24[a,b]	2.46[a,b]
PASSERIFORMES										
Corvus frugilegus	HbA	0.06			5.60	1.50				
	HbD	0.04			4.15	1.46				

Troglodytes aedon	HbA	0.30	2.80	1.48	4.57	1.91	33.90	1.98	25.87	2.11
	HbD	0.30	1.58	1.47	2.67	1.92	22.59	2.39	16.28	2.36
Zonotrochia capensis	HbA	0.30	1.44	1.05	2.39	1.08	7.82	0.72	6.82	0.87
	HbD	0.30	0.87	1.18	1.30	1.26	6.64	1.00	4.20	0.92
STRUTHIOFORMES										
Struthio camelus	HbA	0.58			3.55	1.90			32.73[a]	2.85
	HbD	0.58			2.63	1.75			22.90[a]	2.44

[a]Saturating IHP/Hb4 ratio (>20)

[b]These values are taken from Table 3 (MWC parameters) refer to 25ºC.

Table 6. O_2-affinity differences between avian HbA and HbD isoforms in the absence of allosteric effectors ('stripped') and in the presence of IHP. IHP was present at saturating concentrations (IHP/Hb_4 ratio >20), except where indicated.

Species	**$\Delta\log P_{50}$ (HbA - HbD)**		**T°C**	**pH**	**Buffer**	**Reference**
	Stripped/+KCl	**+IHP**				
ACCIPITRIFORMES						
Gyps fulvus	-0.37[a]	0.06[a]	37	7.4	0.1 M NaHepes/0.1 M KCl	Present study
	-0.41[b]	-	37	7.4	0.1 M NaHepes/0.1 M KCl	Present study
Gyps ruppellii	0.20[a]	~0.40[a]	38	7.5	0.1 M NaHepes/0.1 M KCl	Weber *et al.* (1988)
	0.09[b]	~0.20[b]	38	7.5	0.1 M NaHepes/0.1 M KCl	Weber *et al.* (1988)
Trigonoceps occipitalis	0.10	0.06	38	7.5	0.1 M NaHepes/0.1 M KCl	Hiebl *et al.* (1989)
ANSERIFORMES						
Anas platyrhinchos	-0.32	0.45[c]	20	7.0	0.025 M TrisHCl/0.1 M NaCl	Vandecasserie *et al.* (1973)
Anser anser	-	0.17	37	7.4	0.1 M NaHepes/0.1 M KCl	Present study
Apus apus	0.23	0.54	38	7.5	0.02 M TrisHCl/0.1 M NaCl	Nothum *et al.* (1989)
APODIFORMES						
Amazilia amazilia	-0.03	0.11	37	7.4	0.1 M NaHepes/0.1 M KCl	Present study
Amazilia viridicauda	-0.03	0.12	37	7.4	0.1 M NaHepes/0.1 M KCl	Present study
Coeligena violifer	-0.07	0.12	37	7.4	0.1 M NaHepes/0.1 M KCl	Present study
Patagona gigas	0.01	0.24	37	7.4	0.1 M NaHepes/0.1 M KCl	Present study
Phaethornis malaris	-0.03	0.15	37	7.4	0.1 M NaHepes/0.1 M KCl	Present study
CHARADRIIFORMES						
Catharacta maccormicki	0.20	~0.15	37	7.5	0.1 M NaHepes /0.1 M NaCl	Tamburrini *et al.* (2000)
GALLIFORMES						
Gallus gallus	0.14	0.61[c]	20	7.0	0.025 M TrisHCl/0.1 M NaCl	Vandecasserie *et al.* (1973)
	0.55	0.88	25	7.0	0.1 M NaHepes/0.1 M KCl	Weber *et al.* (2004)

Meleagris gallopavo	-0.27	0.35[c]	20	7.0	0.025 M TrisHCl/0.1 M NaCl	Vandecasserie *et al.* (1973)
Phasianus colchicus	-0.37	0.20[c]	20	7.0	0.025 M TrisHCl/0.1 M NaCl	Vandecasserie *et al.* (1973)
	0.01	-	37	7.4	0.1 M NaHepes/0.1 M KCl	Present study
	0.07	0.09	25	7.5	0.1 M NaHepes/0.1 M KCl	Present study
PASSERIFORMES						
Corvus frugilegus	0.13	-	37	7.4	0.1 M NaHepes/0.1 M KCl	Present study
Troglodytes aedon	0.25	0.18	37	7.4	0.1 M NaHepes/0.1 M KCl	Present study
Zonotrichia capensis	0.22	0.07	37	7.4	0.1 M NaHepes/0.1 M KCl	Present study
PHOENICOPTERIFORMES						
Phoenicopterus roseus	0.24	~0.50	20	7.5	0.05 M TrisHCl/0.1 M NaCl	Sanna *et al.* (2007)
STRUTHIONIFORMES						
Struthio camelus	0.30	0.48[c]	37	7.4	0.05 M TrisHCl/0.2 M NaCl	Oberthur *et al.* (1983)
	0.13	0.16	37	7.4	0.1 M NaHepes/0.1 M KCl	Present study

Table 7. Parameter estimates derived from O_2 equilibrium measurements of pheasant HbA and HbD under the two state Monod-Wyman-Changeux (MWC) allosteric model (cf. Figure 3). In separate analyses, the number of O_2 binding sites was freely estimated (q = free) or fixed at 4 (q = 4).

isoHb	T°C	pH	IHP/Hb_4	P_{50} torr	n_{50}	n_{max}	P_m torr	K_T $torr^{-1}$ (± s.e.m.)	K_R $torr^{-1}$ (± s.e.m.)	L	ΔG kJ mol^{-1}	q
HbA												
q=free												
	25	7.487	--	4.13	2.60	2.63	3.89	0.0663 ± 0.0054	2.0777 ± 0.3396	1.3×10^4	8.38	4.54
	25	7.050	--	7.12	2.61	2.65	6.73	0.0316 ± 0.0008	2.1798 ± 0.1974	3.5×10^4	10.10	3.89
fixed q=4												
	25	7.487	--	4.12	2.44	2.47	3.9	0.0637 ± 0.0046	2.4835 ± 0.3419	8.8×10^3	8.74	4.00
	25	7.050	--	7.13	2.64	2.68	6.73	0.0320 ± 0.0007	2.0496 ± 0.1014	3.6×10^4	9.99	4.00
HbD												
q=free												
	25	7.492	--	3.51	2.47	2.49	3.36	0.0752 ± 0.0042	2.0168 ± 0.1706	4.2×10^3	7.99	4.36
	25	7.496	23.5	26.14	2.71	3.02	22.05	0.0162 ± 0.0008	1.2308 ± 0.8497	7.5×10^7	10.20	5.49
	37	7.433	--	6.05	2.10	2.12	5.72	0.0575 ± 0.0046	1.0665 ± 0.2236	1.7×10^3	7.070	4.10
fixed q=4												
	25	7.492	--	3.50	2.38	2.39	3.36	0.0721 ± 0.0034	2.1948 ± 0.1497	3.0×10^3	8.20	4.00
	25	7.496	23.5	24.2	2.46	2.61	21.5	0.0143 ± 0.0010	$2.7\times10^5 \pm 3.6\times10^{10}$	1.1×10^{27}	11.70	4.00
	37	7.433	--	6.05	2.08	2.10	5.72	0.0572 ± 0.0037	1.1053 ± 0.1196	1.6×10^3	7.12	4.00

Table 8. Posterior probabilities constructed for each functionally divergent site of the four pertinent ancestral sequences.

Site	I	II	III	IV
1	V(0.628)	V(1.000)	V(0.628)	null
5	E(0.969)	A(0.650)	E(0.968)	E(0.876)
8	A(0.988)	T(1.000)	A(0.986)	K(0.998)
9	N(0.325)	N(1.000)	A(0.344)	L(1.000)
11	K(0.972)	K(1.000)	K(0.918)	Q(1.000)
12	A(0.953)	G(1.000)	A(0.892)	Q(1.000)
15	G(0.999)	S(0.996)	G(0.999)	E(1.000)
18	A(0.981)	G(0.996)	A(0.983)	A(0.999)
21	A(0.999)	A(1.000)	A(0.998)	Q(1.000)
28	A(1.000)	T(1.000)	A(1.000)	A(1.000)
30	E(0.998)	E(1.000)	E(0.999)	E(0.998)
50	P(0.630)	H(1.000)	P(0.630)	P(0.815)
53	A(0.999)	A(1.000)	A(0.998)	E(0.953)
57	A(0.859)	A(1.000)	A(0.859)	G(0.999)
67	G(0.998)	V(0.900)	G(1.000)	G(1.000)
68	E(0.997)	E(1.000)	E(0.996)	N(1.000)
71	K(0.690)	N(1.000)	K(0.881)	K(1.000)
72	H(0.947)	H(1.000)	H(0.943)	S(0.838)
75	D(0.843)	D(1.000)	D(0.772)	N(1.000)
77	S(0.480)	A(1.000)	S(0.517)	S(1.000)
78	G(0.994)	G(1.000)	G(0.993)	Q(1.000)
82	K(0.992)	K(1.000)	K(0.991)	E(1.000)
85	D(0.985)	D(1.000)	D(0.984)	N(1.000)
89	Y(0.991)	Q(1.000)	Y(0.997)	Y(1.000)
90	N(0.935)	K(1.000)	N(0.979)	N(1.000)
102	S(0.997)	G(1.000)	S(0.999)	S(1.000)

106	L(0.996)	L(1.000)	L(0.977)	Q(1.000)
113	F(0.926)	H(1.000)	F(0.926)	L(0.999)
114	P(1.000)	P(1.000)	P(1.000)	G(1.000)
115	N(0.373)	S(1.000)	N(0.370)	K(0.998)
116	D(0.630)	A(0.996)	D(0.630)	E(0.861)
117	F(0.998)	L(1.000)	F(0.996)	Y(1.000)
124	A(0.800)	S(1.000)	A(0.891)	A(1.000)
125	L(0.710)	L(1.000)	L(0.435)	Y(0.825)
130	S(0.533)	C(1.000)	S(0.543)	S(0.997)
133	S(0.913)	G(1.000)	S(0.913)	A(0.998)
134	T(0.489)	T(1.000)	T(0.443)	A(0.997)
137	T(0.990)	T(1.000)	T(0.990)	A(1.000)
138	E(0.889)	A(1.000)	E(0.894)	E(1.000)

I	Pre-duplication proto-α
II	Ancestral avian α^A
III	Pre-duplication progenitor of α^D and α^E
IV	Ancestral avian α^D

Table 9. Predicted IHP binding affinities for the α- and β-chain polyphosphate binding sites in homology-based models of pheasant HbA and HbD.

IsoHb	IHP binding site	IHP binding energy (kcal/mol)
HbA	α-chain[a]	-5.1
	β-chain[b]	-6.1
HbD	α-chain[a]	-6.6
	β-chain[b]	-6.2

[a]The 'additional' polyphosphate binding site is formed by seven charged residues at or near the N- and C-termini of the α-chain subunits (sites 1, 95, 99, 134, 137, 138, and 141; Tamburrini *et al.* [2000]).
[b]The main polyphosphate binding site is formed by seven charged residues at or near the N- and C-termini of the β-chain subunits (sites 1, 2, 82, 135, 136, 139, and 143; Tamburrini *et al.* [2000]).

Appendix B.

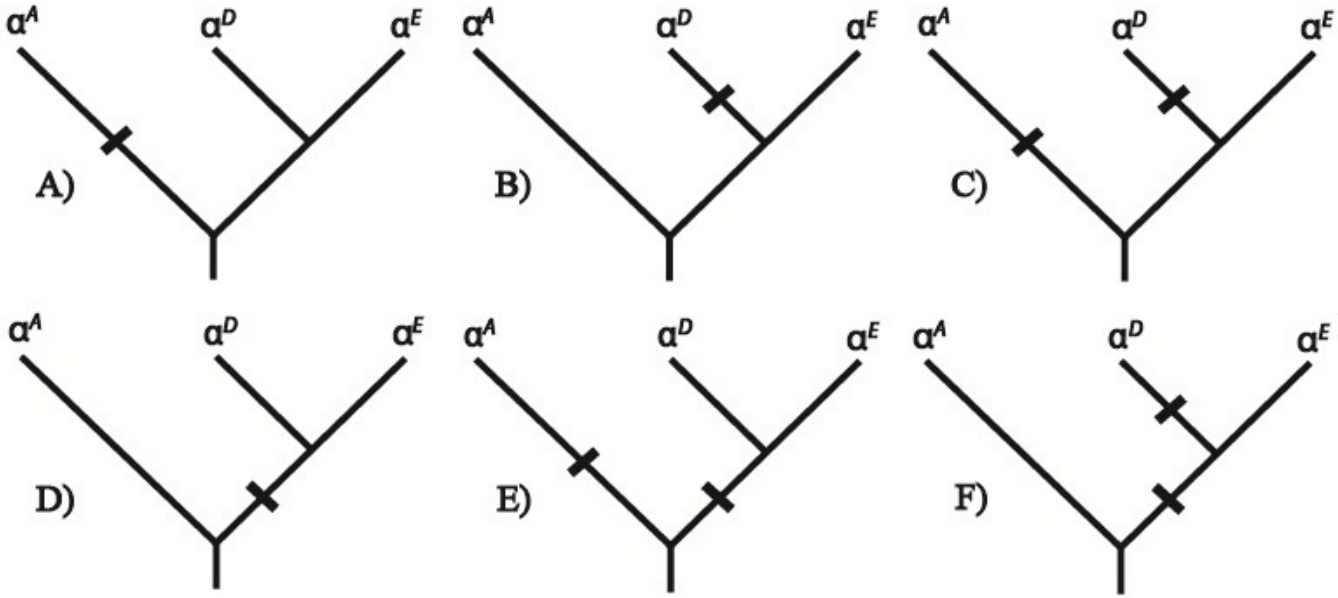

Figure 1. Hypothetical scenarios depicting the phylogenetic distribution of amino acid substitutions that are responsible for functional differentiation between the co-expressed HbA and HbD isoforms in birds. The phylogeny represented in each panel depicts the known branching relationships among the αA-, αD-, and αE-globin genes. At any given site, fixed differences between the αA- and αD-globin genes could be attributable to (A) a substitution that occurred on the branch leading to αA-globin, (B) a substitution that occurred on the post-duplication branch leading to αD-globin, (C) substitutions that occurred on the branch leading to αA-globin and on the post-duplication branch leading to αD-globin, (D) a substitution that occurred on the pre-duplication branch leading to the single-copy progenitor of αD- and αE-globin, (E) substitutions that occurred on the branch leading to αA-globin and on the pre-duplication branch leading to the αD/αE ancestor, or (F) substitutions that occurred on the pre-duplication branch leading to the αD/αE ancestor and on the post-duplication branch leading to αD-globin.

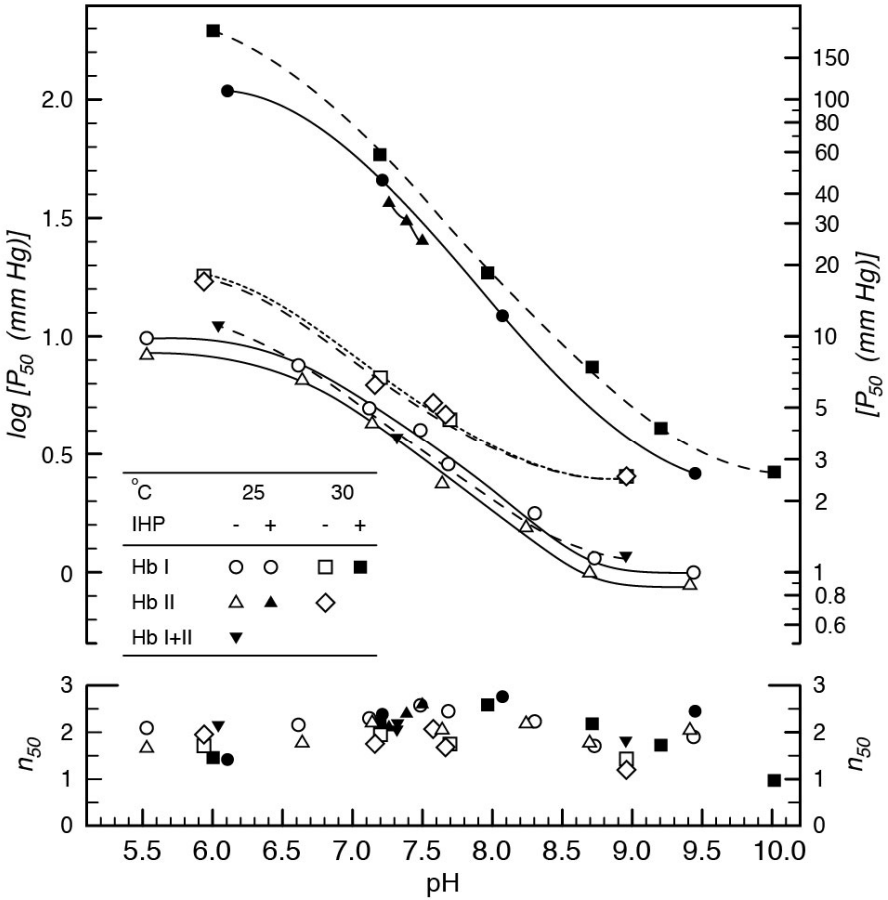

Figure 2. O2 affinity and cooperativity (P50 and n50, respectively) of pheasant HbA and HbD as a function of pH, temperature, and in the absence and presence of IHP (IHP/Hb4 ratio = 23.5). O2 equilibria were measured in 0.1 M NaHEPES buffer containing 0.1 M KCl. Heme concentration, 0.08 mM (HbA) and 0.11 mM (HbD) and 0.10 (HbA +D).

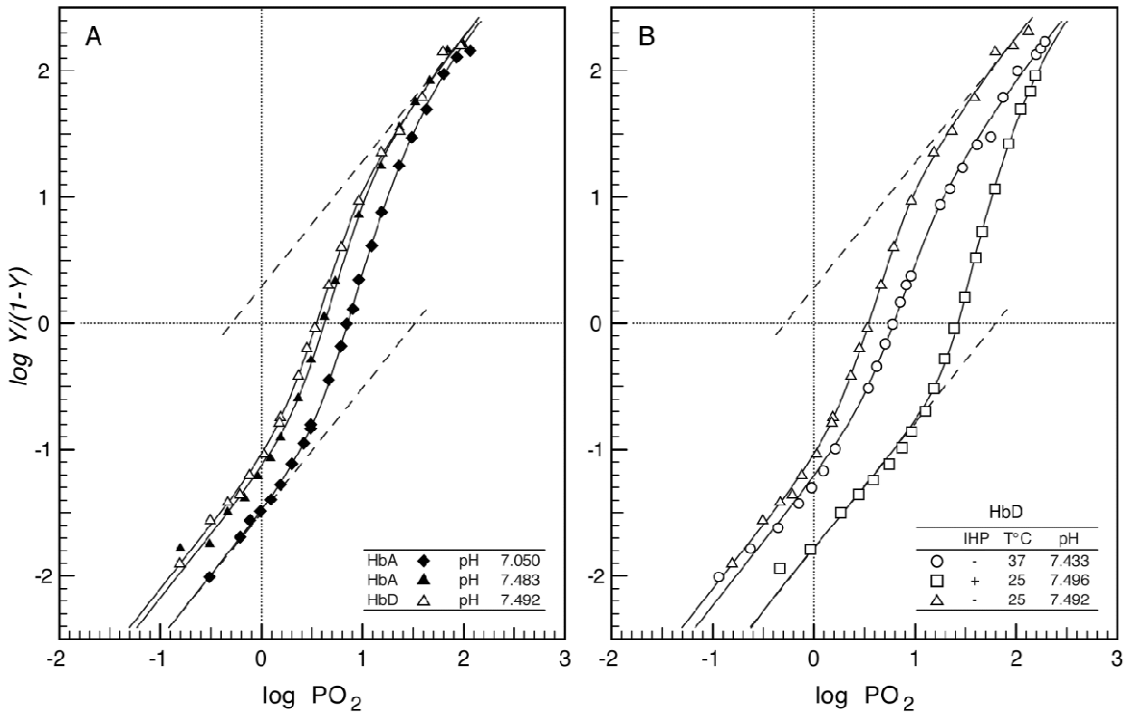

Figure 3. Extended Hill plots of O2 equilibria (where Y = fractional O2 saturation) for pheasant HbA and HbD. (A) HbA and HbD at 25°C; (B) HbD at 25 and 37°C and in the absence and presence of saturating IHP concentration (IHP/Hb ratio = 23.5). In each plot, the intercept of the lower asymptote with the horizontal line at logY/(Y-1) = 0 provides an estimate of KT, the O2 association constant of T-state deoxyHb, and the intercept of the upper asymptote with the same line provides an estimate of KR, the O2 association constant of R-state oxyHb. Heme concentration 0.60 (HbA and HbD); other conditions as described in the legend for Figure 2.

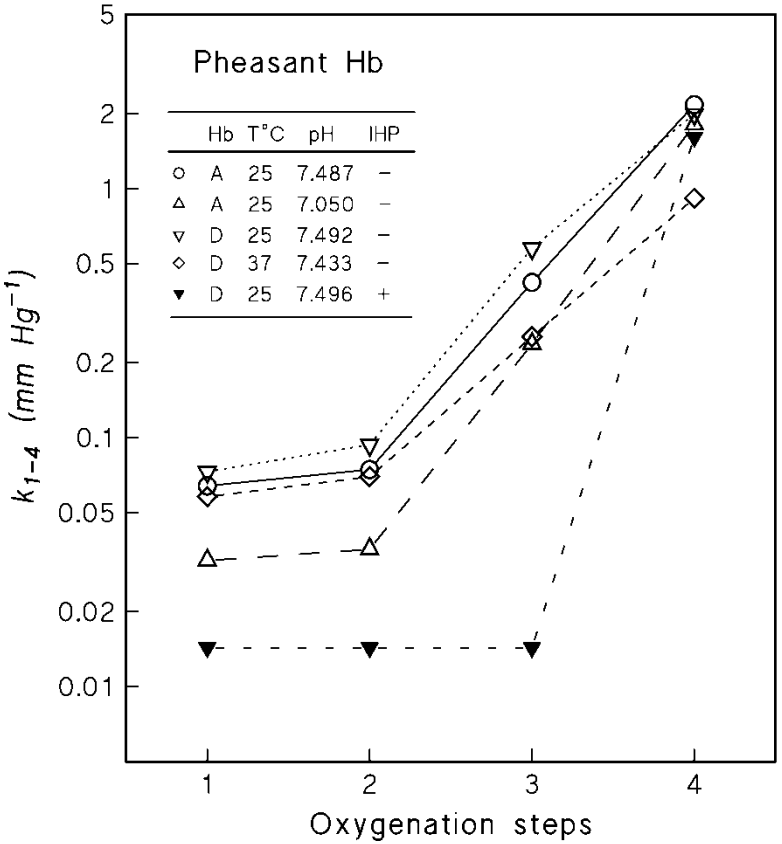

Figure 4. Adair constants (k1, k2, k3, and k4) for pheasant HbA and HbD as a function of temperature, pH, and the absence and presence of IHP (derived from data shown in Figure 2).

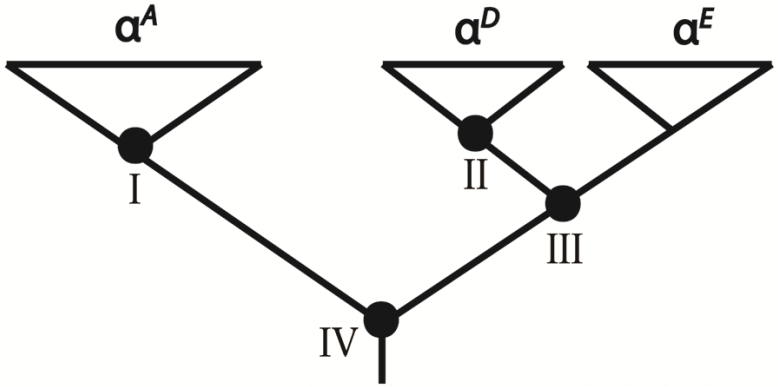

I) Pre-duplication proto-α
II) Ancestral avian α^A
III) Pre-duplication progenitor of α^D and α^E
IV) Ancestral avian α^D

	1	5	8	9	1	1	1	1	2	2	3	5	5	5	6	6	7	7	7	7	8	8	8	9	1 0	1 0	1 1	1 1	1 1	1 1	1 2	1 2	1 3	1 3	1 3	1 3
	1	5	8	9	1	2	5	8	1	8	0	0	3	7	7	8	1	2	5	7	8	2	5	9	0	2	6	3	4	5	6	7	4	5	0	3	4	7	8
I	V	E	A	N	K	A	G	A	A	A	E	P	A	A	G	E	K	H	D	S	G	K	D	Y	N	S	L	F	P	N	D	F	A	L	S	S	T	T	E
II	V	A	T	N	K	G	S	G	A	T	E	H	A	A	V	E	N	H	D	A	G	K	D	Q	K	G	L	H	P	S	A	L	S	L	C	G	T	T	A
III	V	E	A	A	K	A	G	A	A	A	E	P	A	A	G	E	K	H	D	S	G	K	D	Y	N	S	L	F	P	N	D	F	A	L	S	S	T	T	E
IV	-	E	K	L	Q	Q	E	A	Q	A	E	P	E	G	G	N	K	N	N	S	Q	E	N	Y	N	S	Q	L	G	K	D	Y	A	Y	S	A	A	A	E

Figure 5. Reconstructed ancestral states of 39 sites that distinguish the α^A- and α^D-globin polypeptides. As shown in the inset phylogeny of α-like globin genes, ancestral states for each of the 39 sites were reconstructed for 4 separate nodes in the tree. Amino acids are color coded by their distinct physicochemical properties, and are double underscored if the posterior probability < 0.8.

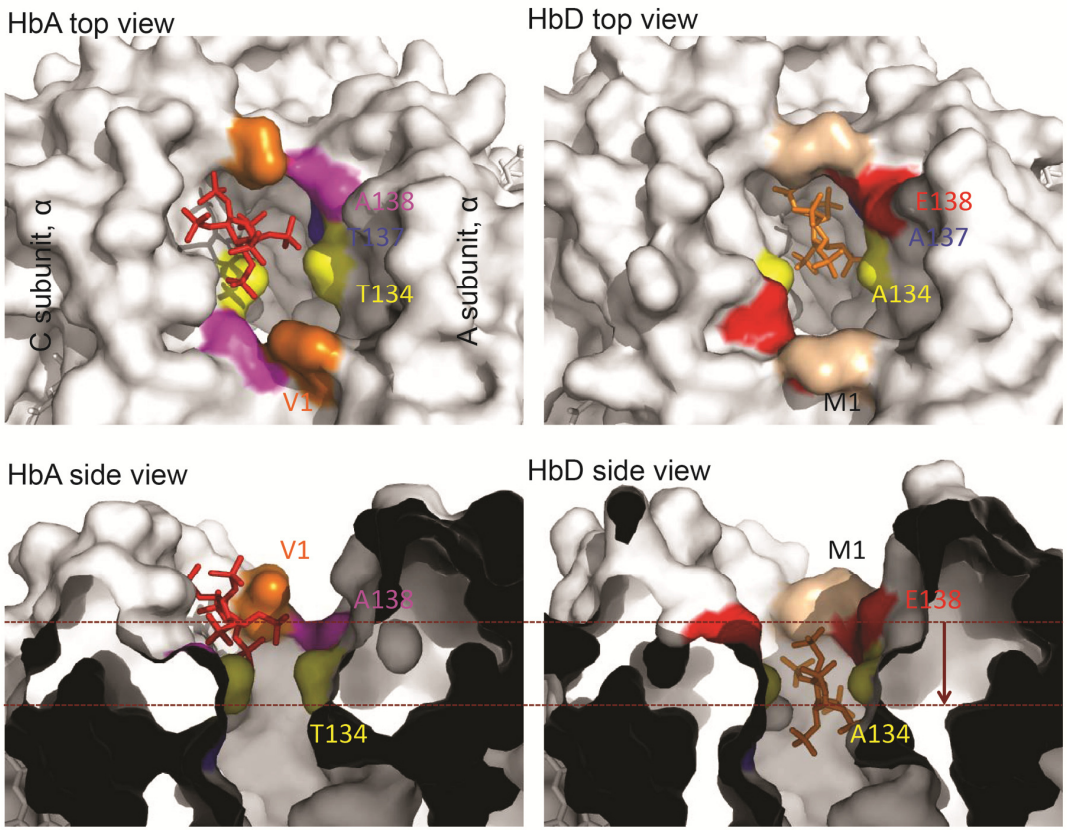

Figure 6. Homology-based structural models of pheasant HbA and HbD showing predicted differences in the stereochemistry of IHP binding between the N- and C-termini of the α-chain subunits.